

Bayesian Multiple Multivariate Density-Density Regression

Khai Nguyen¹, Yang Ni¹, and Peter Mueller^{1,2}

¹Department of Statistics and Data Sciences, University of Texas at Austin

²Department of Mathematics, University of Texas at Austin

January 7, 2026

Abstract

We propose the first approach for multiple multivariate density–density regression (MDDR), making it possible to consider the regression of a multivariate density–valued response on multiple multivariate density–valued predictors. The core idea is to define a fitted distribution using a sliced Wasserstein barycenter (SWB) of push-forwards of the predictors and to quantify deviations from the observed response using the sliced Wasserstein (SW) distance. Regression functions, which map predictors’ supports to the response support, and barycenter weights are inferred within a generalized Bayes framework, enabling principled uncertainty quantification without requiring a fully specified likelihood. The inference process can be seen as an instance of an inverse SWB problem. We establish theoretical guarantees, including the stability of the SWB under perturbations of marginals and barycenter weights, sample complexity of the generalized likelihood, and posterior consistency. For practical inference, we introduce a differentiable approximation of the SWB and a smooth reparameterization to handle the simplex constraint on barycenter weights, allowing efficient gradient-based MCMC sampling. We demonstrate MDDR in an application to inference for population-scale single-cell data. Posterior analysis under the MDDR model in this example includes inference on communication between multiple source/sender cell types and a target/receiver cell type. The proposed approach provides accurate fits, reliable predictions, and interpretable posterior estimates of barycenter weights, which can be used to construct sparse cell-cell communication networks.

Keywords: Sliced Wasserstein Barycenter, Optimal Transport, Single-Cell Data, Generalized Bayes.

1 Introduction

We propose *multiple multivariate density-density regression*, of a *multivariate* density-valued response on several *multivariate* density-valued predictors. The proposed approach does not impose Riemannian geometry on the space of predictors and responses, which is a key requirement for existing density-density regression methods. The proposed approach is computationally and statistically scalable, and can handle predictors and responses of any form, including discrete and continuous. The main feature is the use of a sliced Wasserstein barycenter (Bonneel et al. 2015) (SWB) to define a fitted distribution based on push-forwards of multiple predictors (marginals), and the use of sliced Wasserstein distance (Rabin et al. 2012) (SW) to measure the deviation of the fitted distribution from the observed response distribution. We implement a generalized Bayes (Bissiri et al. 2016) framework for inference on the regression functions, which maps the support of the predictors to that of the response to define the push-forwards, and the barycenter weights. The generalized Bayes setup enables principled belief updating without requiring a fully specified likelihood. While our primary goal is to develop a regression model, the approach can also be interpreted as the first instance of an *inverse SWB* problem, namely, inferring the marginals and their corresponding barycenter weights given a noisy observation of the barycenter.

Beyond the methodological contributions, we establish several theoretical properties of the proposed approach. First, we analyze the stability of SWB by quantifying how it changes when the marginals, the barycenter weights, or both are perturbed. Building on this stability result, we derive two key results: the sample complexity of the generalized likelihood and posterior consistency. Specifically, we show that the generalized likelihood can be reliably estimated even when the distributions are observed only through samples, and we prove consistency of the Bayes estimators of the regression functions and the barycenter weights.

For posterior inference, we develop practicable posterior simulation schemes. First, we

introduce a differentiable approximation of SWB using an iterative algorithm. Second, we handle the simplex constraint on the barycenter weights through a smooth and invertible change-of-variable transformation. Together with the differentiability of SW distance, this makes it possible to use computation-efficient gradient-based Markov chain Monte Carlo (MCMC) samplers, such as the Metropolis-adjusted Langevin algorithm (MALA) ([Girolami & Calderhead 2011](#), [Ning 2025](#)).

Density regression encompasses settings where distribution-valued predictors are used to predict real-valued responses ([Szabó et al. 2016](#), [Matabuena & Petersen 2023](#)), as well as settings where real-valued predictors are used to model distribution-valued responses ([Tokdar et al. 2004](#), [Dunson et al. 2007](#), [Shen & Ghosal 2016](#)). Density-density regression (DDR) generalizes this to scenarios where both the predictor and the response are distributions. For example, simple univariate DDR, with a one-dimensional predictor and a one-dimensional response, is considered in [Zhao et al. \(2023\)](#) using a Riemannian geometry of distributions on the Wasserstein-2 space. The key challenge of extending this approach to multivariate distributions is the computational intractability of Riemannian geometrical tools in higher dimensions. Moreover, the approach also requires distributions to be continuous for accessing the Riemannian structure with the existence of optimal transport maps. To address these limitations, [Nguyen, Ni & Mueller \(2025\)](#) propose a simple multivariate DDR model using the generalized Bayes framework ([Bissiri et al. 2016](#)). The key modeling strategy is to employ the sliced Wasserstein (SW) distance ([Rabin et al. 2012](#)) to construct a generalized likelihood, enabling scalable inference without requiring any Riemannian structure on either the predictors or the responses

Considering more than one predictor gives rise to the multiple regression problem. In the context of DDR, multiple univariate DDR is proposed in [Chen et al. \(2024\)](#). Again, the approach requires the continuity of distributions to utilize the Wasserstein geometry

of distributions that is impractical for computation in multivariate cases. We extend the approach in [Nguyen, Ni & Mueller \(2025\)](#) to the multiple regression setting. First, predictor distributions are transformed to the same dimensions as the response distribution using regression functions. After that, we form the fitted distribution as the SWB of the transformed predictor distributions. An inference model is then defined with a generalized likelihood, based on the SW distance between the fitted distribution and the response.

The use of the SWB and SW distance addresses both of the aforementioned multivariate and finite-sample challenges. One of the results in the upcoming discussion characterizes how the barycenter (prediction) varies with changes in the marginals and barycenter weights. With that, we show that the generalized likelihood achieves a near parametric estimation rate of $\mathcal{O}(n^{-1/2})$ (n is the minimal number of atoms of the involved distributions) under the simple plug-in estimation when the distributions have compact supports. Furthermore, we establish that our model provides consistent Bayesian estimates of the barycenter weights and regression functions under parametric settings. The theoretical studies are novel for both SW literature and the generalized Bayes literature.

Our approach is motivated by the analysis of population-scale single-cell data, where gene expression levels are measured across large numbers of cells sampled from multiple subjects. Because cell types can be reliably identified using established cell markers, these data provide a unique opportunity to uncover communication patterns between cell types through the expression of ligand–receptor pairs. Unlike DDR, which infers communication between pairs of cell types independently, multiple DDR (MDDR) enables joint regression of a target cell type on multiple source cell types simultaneously. Importantly, we only observe a finite (though potentially large) number of cells for each cell type, making the estimation of optimal transport maps, and thus the use of Riemannian geometric tools as in [Chen et al. \(2024\)](#), [Zhu & Müller \(2023\)](#), impractical. In addition, our approach avoids continuity

assumptions on the underlying distributions and is capable of operating beyond Euclidean geometry on atoms of distributions.

With the proposed computational techniques, we are able to perform inference for the MDDR model. We show that the model is particularly meaningful when predictors lie in lower-dimensional spaces than the response, as is typical in single-cell data. The model provides accurate fits and predictions for both simulated and real single-cell datasets. Moreover, the posterior distribution of the barycenter weights enables the construction of a weighted cell-cell communication network. A minor extension of the inference framework by explicitly considering decisions about edge inclusion obtains a sparse network.

The remainder of the article is organized as follows. Section 2 reviews the definitions of Wasserstein distance, SW distance, and the SWB. In Section 3, we introduce the Bayesian MDDR framework, which uses SW and SWB to define a generalized likelihood, establish key theoretical properties, and develop posterior simulation via a MALA sampler. Section 4 presents results on a simulated dataset, highlighting the fundamental difference in the multiple regression under MDR compared to DDR. In Section 5, we apply Bayesian MDDR to single-cell data, exploring fitting, predictive performance, and the discovery of a cell-cell communication network. Section 6 concludes the paper and discusses directions for future work. Technical proofs and additional experimental results are provided in the supplementary material.

For notation, let δ_x denote the Dirac delta measure at x . For any $d \geq 2$, define the unit hypersphere $\mathbb{S}^{d-1} = \{\theta \in \mathbb{R}^d : \|\theta\|_2 = 1\}$. For two sequences a_n and b_n , we write $a_n = \mathcal{O}(b_n)$ if there exists a universal constant C such that $a_n \leq C b_n$ for all $n \geq 1$. Given two measurable spaces $(\mathcal{X}_1, \Sigma_1)$ and $(\mathcal{X}_2, \Sigma_2)$, a measurable function $f : \mathcal{X}_1 \rightarrow \mathcal{X}_2$, and a measure μ on $(\mathcal{X}_1, \Sigma_1)$, the push-forward of μ through f is defined by $f_\sharp \mu(B) = \mu(f^{-1}(B))$, for all $B \in \Sigma_2$. We denote Δ^K as K -simplex i.e., $(\pi_1, \dots, \pi_K) \in \Delta^K$ implies $0 \leq \pi_k \leq 1$, $\forall k = 1, \dots, K$,

and $\sum_{k=1}^K \pi_k = 1$. Additional notation will be introduced as needed.

2 Background

By way of a brief review of Wasserstein distances, sliced Wasserstein distance, and sliced Wasserstein barycenter, we introduce some notation and definitions. Given $p \geq 1$, let $G_1, G_2 \in \mathcal{P}_p(\mathbb{R}^d)$ where $\mathcal{P}_p(\mathbb{R}^d)$ be the set of all distributions supported on \mathbb{R}^d with finite p -th moment. Wasserstein- p distance ([Villani 2009](#), [Peyré & Cuturi 2019](#)) between G_1 and G_2 is defined as:

$$W_p^p(G_1, G_2) = \inf_{\pi \in \Pi(G_1, G_2)} \int_{\mathbb{R}^d \times \mathbb{R}^d} \|x - y\|_p^p d\pi(x, y), \quad (1)$$

where

$$\Pi(G_1, G_2) = \left\{ \pi \in \mathcal{P}(\mathbb{R}^d \times \mathbb{R}^d) \mid \pi(A, \mathbb{R}^d) = G_1(A), \pi(\mathbb{R}^d, B) = G_2(B) \forall A, B \subset \mathbb{R}^d \right\}$$

is the set of all transportation plans/couplings. In one dimension, Wasserstein distance admits the closed-form:

$$W_p^p(G_1, G_2) = \int_0^1 |Q_{G_1}(t) - Q_{G_2}(t)|^p dt, \quad (2)$$

where Q_{G_1} and Q_{G_2} are the quantile function of G_1 and G_2 .

To utilize the closed-form solutions for $d = 1$, sliced Wasserstein (SW) distance is introduced ([Rabin et al. 2012](#), [Nguyen 2025](#)). In particular, SW distance between two distributions $G_1, G_2 \in \mathcal{P}_p(\mathbb{R}^d)$ is defined as:

$$\text{SW}_p^p(G_1, G_2) = \mathbb{E}_{\theta \sim \mathcal{U}(\mathbb{S}^{d-1})} [W_p^p(\theta \sharp G_1, \theta \sharp G_2)], \quad (3)$$

where $\mathcal{U}(\mathbb{S}^{d-1})$ is the uniform distribution over the unit hypersphere in d dimension (\mathbb{S}^{d-1}), and $\theta \sharp G_1$ and $\theta \sharp G_2$ denote the pushforward distribution of G_1 and G_2 through projections $f_\theta(x) = \theta^\top x$. The computation of SW relies on Monte Carlo estimation of the expectation in (3). For example, using simple Monte Carlo estimation:

$$\widehat{SW}_p^p(G_1, G_2; L) = \frac{1}{L} \sum_{l=1}^L W_p^p(\theta_l \sharp G_1, \theta_l \sharp G_2), \quad (4)$$

where $\theta_1, \dots, \theta_L \stackrel{i.i.d.}{\sim} \mathcal{U}(\mathbb{S}^{d-1})$ with L being the number of Monte Carlo samples or the number of projections.

The key benefit of SW compared to Wasserstein distance arises when the distributions are represented by i.i.d. samples. In particular, when observing $x_1, \dots, x_{m_1} \stackrel{i.i.d.}{\sim} G_1$ and $y_1, \dots, y_{m_2} \stackrel{i.i.d.}{\sim} G_2$, we have $\mathbb{E} [\|W_p(\hat{G}_1, \hat{G}_2) - W_p(G_1, G_2)\|] = \mathcal{O}(m_1^{-1/d} + m_2^{-1/d})$ (Fournier & Guillin 2015) and $\mathbb{E} [\|SW_p(\hat{G}_1, \hat{G}_2) - SW_p(G_1, G_2)\|] = \mathcal{O}(m_1^{-1/2} + m_2^{-1/2})$ (Nadjahi et al. 2020, Nietert et al. 2022) where $d > 1$ is the dimension, and $\hat{G}_1 = \frac{1}{m_1} \sum_{i=1}^{m_1} \delta_{x_i}$ and $\hat{G}_2 = \frac{1}{m_2} \sum_{j=1}^{m_2} \delta_{y_j}$. In addition to better sample complexity, SW has a lower time complexity $\mathcal{O}\{(m_1 + m_2) \log(m_1 + m_2)\}$ (Peyré et al. 2019) compared to Wasserstein $\mathcal{O}\{(m_1 + m_2)^3 \log(m_1 + m_2)\}$ (Peyré et al. 2019).

SW distance induces a metric on the space of distribution $\mathcal{P}_p(\mathbb{R}^d)$. The notion of weighted average (Fréchet mean) is generalized to the concept of SW barycenter (Bonneel et al. 2015) (SWB). The SWB (Bonneel et al. 2015) of $K \geq 2$ marginals $G_1, \dots, G_K \in \mathcal{P}_p(\mathbb{R}^d)$ with marginal weights $(\pi_1, \dots, \pi_K) \in \Delta^K$ is defined as:

$$SWB_p(G_1, \dots, G_K, \pi_1, \dots, \pi_K) = \operatorname{argmin}_{G \in \mathcal{P}_p(\mathbb{R}^d)} \sum_{k=1}^K \pi_k SW_p^p(G, G_k). \quad (5)$$

We will discuss the computation of SWB in later sections.

3 Multiple Multivariate Bayesian Density-Density Regression

3.1 Proposed Model

We consider the inference problem of regressing a distribution-valued response $G_i \in \mathcal{P}_p(\mathbb{R}^d)$ ($p \geq 1, d \geq 2$) on multiple distribution-valued predictors F_{i1}, \dots, F_{iK} ($K \geq 2$) with $F_{ik} \in \mathcal{P}_p(\mathbb{R}^{h_k})$ for $k = 1, \dots, K$ and $i = 1, \dots, N$ ($N > 0$). We denote the data as $\mathcal{S} = \{(F_{i1}, \dots, F_{iK}, G_i)\}_{i=1}^N$. We introduce MDDR by way of a *generalized likelihood* (Bissiri et al. 2016) $\ell(f_1, \dots, f_K; G_i, F_{i1}, \dots, F_{iK})$ based on a loss function for a fitted approximation \tilde{G}_i of G_i :

$$\ell(f_1, \dots, f_K, \pi_1, \dots, \pi_K; G_i, F_{i1}, \dots, F_{iK}) = \exp \left\{ -w \text{SW}_p^p[\tilde{G}_i(f, \pi), G_i] \right\}, \quad (6)$$

$$\tilde{G}_i(f, \pi) = \text{SWB}_p(f_1 \# F_{i1}, \dots, f_K \# F_{iK}, \pi_1, \dots, \pi_K), \quad (7)$$

where f_k is a measurable function that maps from \mathbb{R}^{h_k} to \mathbb{R}^d for $k = 1, \dots, K$, $w > 0$, $(\pi_1, \dots, \pi_K) \in \Delta^K$ ($0 \leq \pi_k \leq 1$, $\forall k = 1, \dots, K$, and $\sum_{k=1}^K \pi_k = 1$), and $f_k \# F_{ik}$ denotes the push-forward measure of F_{ik} through f_k .

In (6), \tilde{G}_i is a fitted distribution that represents the (in-sample) prediction of the response distribution G_i given F_{i1}, \dots, F_{iK} . We define \tilde{G}_i as the SWB of random distributions $f_1 \# F_{i1}, \dots, f_K \# F_{iK}$ which we refer to as *pushforwards of predictors*. The fitted distribution \tilde{G}_i can be seen as a Fréchet mean (generalized weighted averaging) of pushforwards of predictors. We then use the SW distance to define a loss function that serves as generalized (negative log) likelihood. The generalized Bayes framework (6) and (7) offers a principled approach for multiple multivariate density-density regression while naturally incorporating uncertainty within a Bayesian framework (priors to be discussed in the next subsection).

The model can be viewed as an instance of a novel inference paradigm, which we refer to as *inverse sliced Wasserstein barycenter*. In particular, we consider the response G_i as a noisy barycenter and aim to infer the underlying marginals and weights that generate it. In our formulation, the barycenter weights π_k are shared across i , and the marginals are constructed through shared regression functions f_k whose inputs are predictor distributions.

To assess goodness of fit, we compute the residual error between the fitted and observed response distributions in (6) and (7): $PE(\mathcal{S}) = \frac{1}{N} \sum_{i=1}^N \text{SW}_p^p(\tilde{G}_i, G_i)$. To calibrate PE , we introduce a reference model that represents a worst-case fit (we introduce specific examples later): $\tilde{G}'_i(f', \pi') = \text{SWB}_p(f'_1 \# F_{i1}, \dots, f'_K \# F_{iK}; 1/K, \dots, 1/K)$, where f' denotes regression functions under strong restrictions. We then normalize the prediction error relative to this reference to obtain the relative residual error (RE):

$$\text{RE}(\mathcal{S}) = \frac{1}{N} \sum_{i=1}^N \frac{\text{SW}_p^p(\tilde{G}_i(f, \pi), G_i)}{\text{SW}_p^p(\tilde{G}'_i(f', \pi'), G_i)}. \quad (8)$$

Here $\text{RE}(\mathcal{S}) = 0$ means a perfect fit as SW is a distance between distributions and $\text{RE}(\mathcal{S}) = 1$ means a poor fit. In practice, we will approximate SW distances using Monte Carlo samples as discussed.

3.2 Likelihood Sample Complexity and Posterior Consistency

We investigate two theoretical aspects of the proposed model. The first result characterizes sample complexity of the generalized likelihood when distributions are represented by i.i.d samples. The second result establishes posterior consistency. In short, with increasing sample size the posterior concentrates around the true parameters under parametric settings of regression functions. In preparation for these results, we first investigate the stability of the SWB, namely, how much the barycenter changes in SW distance under perturbations of the predictors and the barycenter weights.

Lemma 1 (Stability of sliced Wasserstein barycenter). *For any $F_1, \dots, F_K, F'_1, \dots, F'_K \in \mathcal{P}_p(\mathbb{R}^d)$ and $\pi = (\pi_1, \dots, \pi_K) \in \Delta^K, \pi' = (\pi'_1, \dots, \pi'_K) \in \Delta^K$,*

(a) *Let $\bar{F} = SWB_p(F_1, \dots, F_K, \pi)$ and $\bar{F}' = SWB_p(F'_1, \dots, F'_K, \pi)$. Then*

$$SW_p^p(\bar{F}, \bar{F}') \leq \sum_{k=1}^K \pi_k SW_p^p(F_k, F'_k) \leq \max_{k \in \{1, \dots, K\}} SW_p^p(F_k, F'_k). \quad (9)$$

(b) *Let $\bar{F} = SWB_p(F_1, \dots, F_K, \pi)$ and $\bar{F}' = SWB_p(F'_1, \dots, F'_K, \pi')$. Then*

$$SW_p^p(\bar{F}, \bar{F}') \leq 2^{p-1} \left(\sum_{k=1}^K \pi_k SW_p^p(F_k, F'_k) + M \|\pi - \pi'\|_p^p \right), \quad (10)$$

where M is a constant that depends on p and the scale of moments of F'_1, \dots, F'_K .

The proof of Lemma 1 is given in Supplementary Material A.1. Lemma 1(a) shows that when only the marginals are perturbed, the barycenter changes by at most the magnitude of the largest marginal change. Lemma 1(b) states that when both the marginals and their weights are perturbed, the barycenter changes by at most the combined effect of the largest marginal change and the weight change, scaled by a constant depending on the moments of the marginals.

With the stability of SWB, we can discuss a practical aspect of the model. In practice, we usually observe predictors and responses through their samples and have to use an approximation for the (generalized) likelihood in (6). We show that a simple plug-in estimator is suffices.

Theorem 1. *Assume $F_1, \dots, F_K, G \in \mathcal{P}_p(\mathbb{R}^d)$ ($p \geq 1$) have compact supports with diameter $R > 0$, and $\hat{F}_1, \dots, \hat{F}_K, \hat{G}$ are the corresponding empirical distributions with at least n i.i.d support points, $(\pi_1, \dots, \pi_K) \in \Delta^K$, and $\bar{F} = SWB_p(F_1, \dots, F_K, \pi_1, \dots, \pi_K)$ and $\hat{F} =$*

$SWB_p(\hat{F}_1, \dots, \hat{F}_K, \pi_1, \dots, \pi_K)$. The following inequality holds:

$$\mathbb{E} \left[\left| \exp\{-w SW_p^p(\bar{F}, G)\} - \exp(-w SW_p^p(\hat{F}, \hat{G})) \right| \right] \leq C_{p,w,R} \frac{1}{\sqrt{n}}, \quad (11)$$

where $C_{p,w,R} > 0$ is a constant and depends on R , p , and w .

The proof is given in Supplementary Material A.2 and leverages Lemma 1. Theorem 1 suggests that the empirical estimation of the generalized likelihood converges at the order of $\mathcal{O}(n^{-1/2})$, which is a parametric rate. Note that that the result does not require any continuity assumption on the population distributions F_1, \dots, F_K, G i.e., they can be discrete or continuous.

Next, we discuss posterior consistency. Assume that the push forward functions are indexed by parameters $\phi = (\phi_1, \dots, \phi_K) \in \Phi := \Phi_1 \times \dots, \Phi_K$, as $f_\phi = (f_{1,\phi_1}, \dots, f_{K,\phi_K})$ and investigators are interested in $p(\phi, \pi | \mathcal{S})$.

Recognizing the negative log likelihood in (6) as a loss function we define empirical risk and population risk

$$R_N(\phi, \pi) = \frac{1}{N} \sum_{i=1}^n SW_p^p\{\tilde{G}_i(\phi, \pi), G_i\}, \quad R(\phi, \pi) = \mathbb{E}_{(F_1, \dots, F_K, G) \sim P} [SW_p^p\{\tilde{G}(\phi, \pi), G\}]. \quad (12)$$

We make the following assumptions for posterior consistency.

Let P denote a true generating model for the predictors (F_1, \dots, F_K) and a true response G . That is, P is a hypothetical true process generating possible experiments.

Assumption 1 (Identifiability). *There exists $(\phi_0, \pi_0) \in \Phi \times \Delta^K$ such that $R(\phi, \pi)$ attains its unique minimum at (ϕ_0, π_0) . Moreover, for every $\epsilon > 0$, $\Delta(\epsilon) = \inf_{\{(\phi, \pi) \in \Phi \times \Delta^K : \|\phi - \phi_0\|_p + \|\pi - \pi_0\|_p \geq \epsilon\}} (R(\phi, \pi) - R(\phi_0, \pi_0)) > 0$.*

Assumption 2 (Compactness). *The parameter space Φ is compact.*

Assumption 3 (Bounded moments). *For all $(F_1, \dots, F_K, G) \in \text{supp}(P)$, $\mathbb{E}_{X \sim F_k}[\|X\|_p^p] \leq C_k$, $\mathbb{E}_{Y \sim G}[\|Y\|_p^p] \leq C_G$, for some constants $C_k, C_G < \infty$ for $k = 1, \dots, K$.*

Assumption 4 (Prior positivity). *The prior on p assigns positive mass to every neighborhood of (ϕ_0, π_0) (defined in Assumption 1); that is, for every $\epsilon > 0$, $p(B_\epsilon(\phi_0, \pi_0)) > 0$, where $B_\epsilon(\phi_0, \pi_0) = \{(\phi, \pi) \in \Phi \times \Delta^K : \|\phi - \phi_0\|_p + \|\pi - \pi_0\|_p < \epsilon\}$.*

Assumption 5 (Regularity of Regression Functions). *For any $k = 1, \dots, K$, the regression function f_{k, ϕ_k} admits $\omega_k : \mathbb{R}_+ \rightarrow \mathbb{R}_+$ ($\lim_{t \rightarrow 0} \omega_k(t) = 0$) as a modulus of continuity: $\mathbb{E}_{X \sim F_k} \|f_{k, \phi_k}(X) - f_{k, \phi'_k}(X)\|_p^p \leq \omega_k(\|\phi_k - \phi'_k\|_p^p)$ for all $(F_1, \dots, F_K, G) \in \text{supp}(P)$ and $\phi_k, \phi'_k \in \Phi_k$. For all $k = 1, \dots, K$, $(F_1, \dots, F_K, G) \in \text{supp}(P)$ and $\phi_k \in \Phi_k$, $\mathbb{E}_{X \sim F_k} \|f_{k, \phi_k}(X)\|_p^p \leq C$, for a constant $C < \infty$.*

Theorem 2. *Under Assumptions 1–5, for every $\epsilon > 0$, the posterior measure p_N satisfies*

$$p_N \left(\{(\phi, \pi) \in \Phi \times \Delta^K : \|\phi - \phi_0\|_p + \|\pi - \pi_0\|_p \geq \epsilon\} \right) \xrightarrow{a.s.} 0, \quad (13)$$

as $N \rightarrow \infty$ under i.i.d sampling.

The proof of Theorem 2 is provided in Supplementary Material A.3. In particular, Lemma 1 is instrumental in establishing a uniform law of large numbers for $R_N(\phi, \pi)$, which in turn enables us to prove consistency under stated assumptions.

3.3 Computation of Sliced Wasserstein Barycenter

Before introducing details of posterior inference, we discuss the computation of SWB, which is required for the evaluation of the likelihood in (7). We recall the optimization problem which defines SWB with marginals $G_1, \dots, G_K \in \mathcal{P}_p(\mathbb{R}^d)$ and $\pi \in \Delta^K$:

$$\min_{G \in \mathcal{P}_p(\mathbb{R}^d)} \sum_{k=1}^K \pi_k \text{SW}_p^p(G, G_k) \quad (14)$$

Solving SWB is an optimization problem and is still a developing research direction (Bonneel et al. 2015, Nguyen, Nguyen & Ho 2025). SWB is a convex problem on the space of distributions i.e., the mapping $G \rightarrow \sum_{k=1}^K \pi_k \text{SW}_p^p(G, G_k)$ is convex (Proposition 1 in Supplementary Material A.4). However, in practice we often need to parameterize the barycenter for tractable optimization, which may break convexity.

In our case, we use a plug-in estimator for the generalized likelihood, solving SWB for the empirical distributions $G_1 = \frac{1}{M_{G_1}} \sum_{i=1}^{M_{G_1}} \delta_{x_{i1}}, \dots, G_k = \frac{1}{M_{G_K}} \sum_{i=1}^{M_{G_K}} \delta_{x_{iK}}$. It is then natural to also restrict the barycenter to an empirical distribution, i.e., $G = \frac{1}{M_G} \sum_{\ell=1}^{M_G} \delta_{z_\ell}$ (also known as the free support barycenter (Cuturi & Doucet 2014)) where $z_1, \dots, z_{M_G} \in \mathbb{R}^d$. We update the support points of the barycenter using an iterative procedure with the gradient:

$$\begin{aligned} \nabla_{z_\ell} \sum_{k=1}^K \pi_k \text{SW}_p^p(G, G_k) &= \sum_{k=1}^K \pi_k \nabla_{z_\ell} \text{SW}_p^p(G, G_k) \\ &= \sum_{k=1}^K \pi_k \nabla_{z_\ell} \mathbb{E}_{\theta \sim \mathcal{U}(\mathbb{S}^{d-1})} [W_p^p(\theta \sharp G, \theta \sharp G_k)] \\ &= \sum_{k=1}^K \pi_k \mathbb{E}_{\theta \sim \mathcal{U}(\mathbb{S}^{d-1})} [\nabla_{z_\ell} W_p^p(\theta \sharp G, \theta \sharp G_k)], \end{aligned} \quad (15)$$

for any $z_\ell \in \{z_1, \dots, z_{M_G}\}$. Let $\gamma_{k,\theta}^*$ be the optimal transport plan between $\theta \sharp G$ and $\theta \sharp G_k$, implying

$$\begin{aligned} \nabla_{z_\ell} W_p^p(\theta \sharp G, \theta \sharp G_k) &= \nabla_{z_\ell} \sum_{j=1}^{M_{G_k}} \gamma_{k,\theta,\ell,j}^* |\theta^\top (z_\ell - x_{jk})|^p \\ &= p\theta \sum_{j=1}^{M_{G_k}} \gamma_{k,\theta,\ell,j}^* |\theta^\top (z_\ell - x_{jk})|^{p-2} (\theta^\top (z_\ell - x_{jk})), \end{aligned} \quad (16)$$

when $\theta^\top (z_\ell - x_{jk}) \neq 0$. A general update is of the form:

$$z_\ell^{(t)} = g \left(z_\ell^{(t-1)}, \nabla_{z_\ell^{(t-1)}} \sum_{k=1}^K \pi_k \text{SW}_p^p(G^{(t-1)}, G_k) \right), \quad (17)$$

where $G^{(t)} = \frac{1}{M_G} \sum_{i=1}^{M_G} \delta_{z_\ell^{(t)}}$, $g : \mathbb{R}^d \times \mathbb{R}^d \rightarrow \mathbb{R}^d$ is the update rule, and $z_1^{(0)}, \dots, z_{M_G}^{(0)}$ are randomly initialized. We update $T > 0$ iterations to obtain an approximation $G^{(T)}$ of SWB. Overall, the time complexity is $\mathcal{O}(TM_{max} \log M_{max})$ where $M_{max} = \max\{M_{G_1}, \dots, M_{G_K}, M_G\}$.

For the upcoming discussion of efficient posterior inference we will use the Jacobian $\frac{\partial z_\ell^{(T)}(\phi)}{\partial \phi}$. Specifically, let $f_\phi = (f_{1,\phi_1}, \dots, f_{k,\phi_k})$ be parametric regression functions with $\phi = (\phi_1, \dots, \phi_K)$, $G_1 = \frac{1}{M_{G_1}} \sum_{i=1}^{M_{G_1}} \delta_{f_{1,\phi_1}(x_{i1})}, \dots, G_k = \frac{1}{M_{G_K}} \sum_{i=1}^{M_{G_k}} \delta_{f_{k,\phi_K}(x_{iK})}$. We consider the Jacobian matrix $\frac{\partial z_\ell^{(T)}(\phi)}{\partial \phi}$, which is a function of ϕ . Let $h_\ell^{(t-1)}(\phi) = \nabla_{z_\ell^{(t-1)}} \sum_{k=1}^K \pi_k \text{SW}_p^p(G^{(t-1)}, G_k)$ (see (15)-(16)). By the update rule, we have $z_\ell^{(T)}(\phi) = g(z_\ell^{(T-1)}(\phi), h_\ell^{(T-1)}(\phi))$. The Jacobian can be written as:

$$\frac{\partial z_\ell^{(T)}(\phi)}{\partial \phi} = \frac{\partial z_\ell^{(T)}(\phi)}{\partial z_\ell^{(T-1)}(\phi)} \frac{\partial z_\ell^{(T-1)}(\phi)}{\partial \phi} + \frac{\partial z_\ell^{(T)}(\phi)}{\partial h_\ell^{(T-1)}(\phi)} \frac{\partial h_\ell^{(T-1)}(\phi)}{\partial \phi}, \quad (18)$$

where $\frac{\partial z_\ell^{(T)}(\phi)}{\partial z_\ell^{(T-1)}(\phi)}$ and $\frac{\partial z_\ell^{(T)}(\phi)}{\partial h_\ell^{(T-1)}(\phi)}$ depend on the update rule g (the exact form for a specific g will be provided later), $\frac{\partial z_\ell^{(T-1)}(\phi)}{\partial \phi}$ can be computed recursively, and

$$\begin{aligned} \frac{\partial h_\ell^{(T-1)}(\phi)}{\partial \phi} &= \frac{\partial}{\partial \phi} \left(\sum_{k=1}^K \pi_k \mathbb{E} \left[p \theta \sum_{j=1}^{M_{G_k}} \gamma_{k,\theta,\ell j}^{\star(T-1)} \left| \theta^\top (z_\ell^{(T-1)}(\phi) - f_{k,\phi_k}(x_{jk})) \right|^{p-2} \right. \right. \\ &\quad \left. \left. \left(\theta^\top (z_\ell^{(T-1)}(\phi) - f_{k,\phi_k}(x_{jk})) \right) \right] \right) \\ &= \sum_{k=1}^K \pi_k \mathbb{E} \left[p(p-1) \theta \sum_{j=1}^{M_{G_k}} \gamma_{k,\theta,\ell j}^{\star(T-1)} \left| \theta^\top (z_\ell^{(T-1)}(\phi) - f_{k,\phi_k}(x_{jk})) \right|^{p-2} \right. \\ &\quad \left. \left(\theta^\top \left(\frac{\partial z_\ell^{(T-1)}(\phi)}{\partial \phi} - \frac{\partial f_{k,\phi_k}(x_{jk})}{\partial \phi} \right) \right) \right], \end{aligned} \quad (19)$$

where $\gamma_{k,\theta}^{\star(T-1)}$ be the optimal transport plan between $\theta \sharp G^{(T-1)}$ and $\theta \sharp G_k$. In the above, the expectation is with respect to $\theta \sim \mathcal{U}(\mathbb{S}^{d-1})$, $\gamma_{\theta,\ell j}^{\star(T-1)}$ is the optimal transport plan between $\theta \sharp G^{(T-1)}$ and $\theta \sharp G_k$, and $\frac{\partial f_{k,\phi_k}(x_{jk})}{\partial \phi}$ depends on the parameterization of the regression function f_{k,ϕ_k} which will be discussed later.

Similarly, we will also need $\frac{\partial z_\ell^{(T)}(\pi)}{\partial \pi}$, which can be derived as:

$$\frac{\partial z_\ell^{(T)}(\pi)}{\partial \pi} = \frac{\partial z_\ell^{(T)}(\pi)}{\partial z_\ell^{(T-1)}(\pi)} \frac{\partial z_\ell^{(T-1)}(\pi)}{\partial \pi} + \frac{\partial z_\ell^{(T)}(\pi)}{\partial h_\ell^{(T-1)}(\pi)} \frac{\partial h_\ell^{(T-1)}(\pi)}{\partial \pi}, \quad (20)$$

where $\frac{\partial z_\ell^{(T)}(\pi)}{\partial z_\ell^{(T-1)}(\pi)}$ and $\frac{\partial z_\ell^{(T)}(\pi)}{\partial h_\ell^{(T-1)}(\pi)}$ depend on the update rule g , $\frac{\partial z_\ell^{(T-1)}(\pi)}{\partial \pi}$ can be computed recursively, and

$$\begin{aligned} \frac{\partial h_\ell^{(T-1)}(\pi)}{\partial \pi} &= \frac{\partial}{\partial \pi} \left(\sum_{k=1}^K \pi_k \mathbb{E} \left[p \theta \sum_{j=1}^{M_{G_k}} \gamma_{k,\theta,\ell j}^{\star,(T-1)} \left| \theta^\top (z_\ell^{(T-1)}(\pi) - f_{k,\phi_k}(x_{jk})) \right|^{p-2} \right. \right. \\ &\quad \left. \left. \left(\theta^\top (z_\ell^{(T-1)}(\pi) - f_{k,\phi_k}(x_{jk})) \right) \right] \right) = (\mathcal{G}_1, \dots, \mathcal{G}_K), \end{aligned} \quad (21)$$

with

$$\begin{aligned} \mathcal{G}_k &= \mathbb{E} \left[p \theta \sum_{j=1}^{M_{G_k}} \gamma_{k,\theta,\ell j}^{\star,(T-1)} \left| \theta^\top (z_\ell^{(T-1)}(\pi) - f_{k,\phi_k}(x_{jk})) \right|^{p-2} \left(\theta^\top (z_\ell^{(T-1)}(\pi) - f_{k,\phi_k}(x_{jk})) \right) \right] \\ &\quad + \sum_{k=1}^K \pi_k \mathbb{E} \left[p(p-1) \sum_{j=1}^{M_{G_k}} \gamma_{k,\theta,\ell j}^{\star,(T-1)} \left| \theta^\top (z_\ell^{(T-1)}(\pi) - f_{k,\phi_k}(x_{jk})) \right|^{p-2} \theta \theta^\top \right] \frac{\partial z_\ell^{(T-1)}(\pi)}{\partial \pi_k}. \end{aligned} \quad (22)$$

In practice, we use Monte Carlo samples $\theta_1, \dots, \theta_L \stackrel{i.i.d.}{\sim} \mathcal{U}(\mathbb{S}^{d-1})$ to approximate the expectation in the gradients. For the update rule g , we use Adam (Kingma & Ba 2014), which can be described as:

$$\begin{aligned} z_\ell^{(t)} &= g(z_\ell^{(t-1)}, h_\ell^{(t-1)}) = z_\ell^{(t-1)} - \eta \frac{\hat{m}_i^{(t)}}{\sqrt{\hat{v}_i^{(t)}} + \epsilon}, \\ \hat{m}_i^{(t)} &= \frac{m_i^{(t)}}{1 - \beta_1^t}, \quad \hat{v}_i^{(t)} = \frac{v_i^{(t)}}{1 - \beta_2^t}, \\ m_i^{(t)} &= \beta_1 m_i^{(t-1)} + (1 - \beta_1) h_i^{(t-1)}, \quad v_i^{(t)} = \beta_2 v_i^{(t-1)} + (1 - \beta_2) (h_i^{(t-1)})^2. \end{aligned} \quad (23)$$

where $\eta > 0$ is the step size, $\beta_1 \in [0, 1]$ and $\beta_2 \in [0, 1]$ are momentum parameters, $\epsilon > 0$ for

avoiding 0 in the denominator. For this update rule, we have:

$$\frac{\partial z_\ell^{(t)}}{\partial z_\ell^{(t-1)}} = I, \quad \frac{\partial z_\ell^{(t)}}{\partial h_\ell^{(t-1)}} = -\eta \text{diag} \left(\frac{\partial \hat{m}_i^{(t)}}{\partial h_\ell^{(t-1)}} \frac{1}{\sqrt{\hat{v}_i^{(t)}} + \epsilon} + \hat{m}_i^{(t)} \frac{\partial \left(\sqrt{\hat{v}_i^{(t)}} + \epsilon \right)^{-1}}{\partial h_\ell^{(t-1)}} \right), \quad (24)$$

where

$$\frac{\partial \hat{m}_i^{(t)}}{\partial h_\ell^{(t-1)}} = \frac{1 - \beta_1}{1 - \beta_1^t} I, \quad \frac{\partial \left(\sqrt{\hat{v}_i^{(t)}} + \epsilon \right)^{-1}}{\partial h_\ell^{(t-1)}} = -\frac{1}{\left(\sqrt{\hat{v}_i^{(t)}} + \epsilon \right)^2} \frac{1}{2\sqrt{\hat{v}_i^{(t)}}} \frac{\partial \hat{v}_i^{(t)}}{\partial h_\ell^{(t-1)}}, \quad (25)$$

$$\frac{\partial \hat{v}_i^{(t)}}{\partial h_\ell^{(t-1)}} = \frac{2(1 - \beta_2)}{1 - \beta_2^t} \text{diag}(h_\ell^{(t-1)}). \quad (26)$$

We note that there is room to improve the update rule, for example by using a Riemannian Silver step size (Park et al. 2025). However, we keep the update rule as simple as possible while retaining good practical performance. we now can discuss posterior inference in the next section.

3.4 Posterior Inference

The generalized posterior is given by:

$$p(f, \pi \mid \mathcal{S}) \propto p(f, \pi) \prod_{i=1}^N \ell(f_1, \dots, f_K, \pi_1, \dots, \pi_K; G_i, F_{i1}, \dots, F_{iK}). \quad (27)$$

We implement posterior Markov chain Monte Carlo (MCMC) simulation using Metropolis-Hastings (MH) transition probabilities with proposals to mimic $p(f \mid \pi, \mathcal{S})$ and $p(\pi \mid f, \mathcal{S})$. In particular, we construct proposals $f^* \sim q(f^* \mid f)$ and $\pi^* \sim q(\pi^* \mid \pi)$, and accept proposed samples with the probabilities:

$$\min \left\{ 1, \frac{p(f^* \mid \pi, \mathcal{S})q(f \mid f^*)}{p(f \mid \pi, \mathcal{S})q(f^* \mid f)} \right\}, \quad \min \left\{ 1, \frac{p(\pi^* \mid f, \mathcal{S})q(\pi \mid \pi^*)}{p(\pi \mid f, \mathcal{S})q(\pi^* \mid \pi)} \right\}. \quad (28)$$

In practice, we only observe i.i.d samples from distributions. Therefore, we need to approximate the generalized likelihood for computing the acceptance-rejection probability. Using the empirical distributions we have:

$$\begin{aligned} & \ell(f_1, \dots, f_K, \pi_1, \dots, \pi_K; G_i, F_{i1}, \dots, F_{iK}) \\ & \approx \ell(f_1, \dots, f_K, \pi_1, \dots, \pi_K; \hat{G}_i, \hat{F}_{i1}, \dots, \hat{F}_{iK}) = \exp \left\{ -w \text{SW}_p^p \left[\hat{\tilde{G}}_i(f, \pi), \hat{G}_i \right] \right\}, \end{aligned} \quad (29)$$

where $\hat{\tilde{G}}_i(f, \pi) = \text{SWB}_p(f_1 \# \hat{F}_{i1}, \dots, f_K \# \hat{F}_{iK}, \pi_1, \dots, \pi_K)$, and $\hat{G}_i, \hat{F}_{i1}, \dots, \hat{F}_{iK}$ are empirical distributions of $G_i, F_{i1}, \dots, F_{iK}$. As stated in Theorem 1, this approximation converges well. Next, we approximate the SWB as discussed before (Section 3.3), approximating $\hat{\tilde{G}}_i(f, \pi)$ by $\hat{\tilde{G}}_i^{(T)}(f, \pi)$ for $T > 0$. We denote the approximated generalized likelihood as:

$$\hat{\ell}(f_1, \dots, f_K, \pi_1, \dots, \pi_K; G_i, F_{i1}, \dots, F_{iK}, T) = \exp \left\{ -w \text{SW}_p^p \left[\hat{\tilde{G}}_i^{(T)}(f, \pi), \hat{G}_i \right] \right\}. \quad (30)$$

Updating ϕ : We now discuss the construction of the proposal distributions for ϕ and π , respectively. We parameterize the regression function f_ϕ as $f_\phi = (f_{1,\phi_1}, \dots, f_{K,\phi_K})$ with $\phi = (\phi_1, \dots, \phi_K)$. We use a MALA proposal $q(\phi^* \mid \phi) \propto \exp \left(-\frac{1}{4\eta_1} \|\phi^* - \phi - \eta_1 \nabla_\phi \log \hat{p}(\phi \mid \pi, \mathcal{S})\|_2^2 \right)$, for a fixed step size $\eta_1 > 0$, and

$$\begin{aligned} \nabla_\phi \log p(\phi \mid \pi, \mathcal{S}) & \approx \nabla_\phi \log p(\phi) - w \sum_{i=1}^N \nabla_\phi \mathbb{E} \left\{ W_p^p \left[\theta \# \hat{\tilde{G}}_i^{(T)}(\phi, \pi), \theta \# \hat{G}_i \right] \right\}, \\ & = \nabla_\phi \log p(\phi) - w \sum_{i=1}^N \mathbb{E} \left\{ \nabla_\phi W_p^p \left[\theta \# \hat{\tilde{G}}_i^{(T)}(\phi, \pi), \theta \# \hat{G}_i \right] \right\}. \end{aligned} \quad (31)$$

Let $\psi_{i,\theta}^*$ be the optimal transport plan between $\theta \# \hat{\tilde{G}}_i^{(T)}(\phi, \pi)$ and $\theta \# \hat{G}_i$, M_i be the number of

atoms of $\tilde{G}_i^{(T)}(\phi, \pi)$, we have:

$$\nabla_\phi W_p^p(\theta \sharp \tilde{G}_i^{(T)}(\phi, \pi), \theta \sharp \hat{G}_i) = \nabla_\phi \sum_{j=1}^{M_i} \sum_{j'=1}^{M_{G_i}} \psi_{i, \theta, jj'}^\star |\theta^\top(z_{i,j}^{(T)}(\phi, \pi) - y_{i,j'})|^p \quad (32)$$

$$= p \sum_{j=1}^{M_i} \sum_{j'=1}^{M_{G_i}} \psi_{i, \theta, jj'}^\star |\theta^\top(z_{i,j}^{(T)}(\phi, \pi) - y_{i,j'})|^{p-2} (\theta^\top(z_{i,j}^{(T)}(\phi, \pi) - y_{i,j'})) \\ \left(\frac{\partial z_{i,j}^{(T)}(\phi, \pi)}{\partial \phi} \right)^\top \theta, \quad (33)$$

where $\frac{\partial z_{i,j}^{(T)}(\phi, \pi)}{\partial \phi}$ is discussed in Section 3.3. We sample $\phi^* \sim q(\phi^* \mid \phi)$ as $\phi^* = \phi + \eta_1 \nabla_\phi \log p(\phi \mid \pi, \mathcal{S}) + \sqrt{2\eta_1} \epsilon_0$, with $\epsilon_0 \sim \mathcal{N}(0, I)$, a standard multivariate Gaussian distribution of dimension matching the parameter ϕ .

Updating π : To construct a gradient based transition probability for π we use a change of variables to remove the simplex constraint of π :

$$\pi_k = \frac{e^{\varpi_k}}{1 + \sum_{k'=1}^{K-1} e^{\varpi_{k'}}} \quad \text{for } k = 1, \dots, K-1, \quad \pi_K = \frac{1}{1 + \sum_{k'=1}^{K-1} e^{\varpi_{k'}}}. \quad (34)$$

Let $D = \text{diag}(\pi_1, \dots, \pi_{K-1})$. We have the Jacobian $J = D - \pi \pi^\top$ of the transformation and its determinant: $\det(J) = \det(D(1 - \pi^\top D^{-1} \pi)) = \prod_{k=1}^K \pi_k$, implying $p(\varpi_k) = p(\pi) \prod_{k=1}^K \pi_k$. We use the proposal $q(\varpi^* \mid \varpi) \propto \exp\left(-\frac{1}{4\eta_2} \|\varpi^* - \varpi - \eta_2 \nabla_\varpi \log p(\varpi \mid \phi, \mathcal{S})\|_2^2\right)$, for a fixed step size $\eta_2 > 0$, and

$$\nabla_\varpi \log p(\varpi \mid \phi, \mathcal{S}) = \nabla_\phi \log p(\varpi) - w \sum_{i=1}^N \nabla_\varpi \mathbb{E} \left\{ W_p^p \left[\theta \sharp \tilde{G}_i^{(T)}(\phi, \varpi), \theta \sharp \hat{G}_i \right] \right\}, \quad (35)$$

which can be derived with the gradient $\frac{\partial z_{i,j}^{(T)}(\phi, \pi)}{\partial \pi}$ as discussed in Section 3.3. Since ϖ and π are connected through invertible deterministic mappings, sampling for ϖ implies sampling for π .

3.5 A Parsimonious Model

We specify a parsimonious model, which we will further use for later simulation and real data analysis. First, we use a linear parameterization for regression functions:

$$f_{k,\phi_k}(x) = f_{k,A_k,b_k}(x) = A_k x + b_k, \forall k = 1, \dots, K, \quad (36)$$

where $A_k \in \mathbb{R}^{h \times d_k}$ is the coefficient matrix and $b_k \in \mathbb{R}^h$ is the intercept. As discussed in Nguyen, Ni & Mueller (2025), this type of regression function satisfies Assumption 5 i.e., they satisfy the Lipschitz continuity property. As discussed in Section 3.3 and Section 3.4, we use $\frac{\partial f_{k,A_k,b_k}(x)}{\partial A_k} := I_h \otimes x^\top$ (should be vectorized to match the vector form of ϕ in Section 3.3) and $\frac{\partial f_{k,A_k,b_k}(x)}{\partial b_k} = I_h$ for $k = 1, \dots, K$ for posterior simulation.

We complete the model with a prior on the regression functions:

$$A_k[ij] \sim Laplace(0, 1), b_k[i] \sim \mathcal{N}(0, 10^3), \forall i = 1, \dots, d_k, \forall j = 1, \dots, h, \quad (37)$$

and the barycenter weights:

$$(\pi_1, \dots, \pi_K) \sim Dir(\alpha), \alpha = (0.01, \dots, 0.01), \quad (38)$$

which implies the following prior on ϖ : $p(\varpi) = \frac{1}{B(\alpha_0)} \prod_{k=1}^K \pi_k^{\alpha_k}$. Any alternative family of differentiable functions f_{k,ϕ_k} could be used, such as deep neural networks (Wilson & Izmailov 2020), if desired or required. We adopt the linear form because it is interpretable, parsimonious and, as shown later, sufficiently expressive for our analysis. For RE (8), we select $f'_k(x) = b_k$ i.e., an intercept model.

Model	Train RE	Train RE 95% HCI	Test RE	Test 95% HCI
DDR	0.4097	0.4018-0.4168	0.4448	0.4370-0.4539
MDDR	0.1331	0.078-0.1714	0.1330	0.094-0.1777

Table 1: Comparison of performance between single-predictor DDR models and the multi-predictor MDDR model with simulated data. Reported are training and test relative errors (RE) with their 95% highest credible intervals (HCI).

4 Simulation

We assess the proposed MMDR through a simulation study. In particular, we highlight the benefits of using SWB to generate multi-variate responses from lower-dimensional predictors (in this case, bivariate responses from predictors with 1-dimensional structure).

We first sample $A_1, A_2, A_3 \stackrel{i.i.d.}{\sim} \mathcal{U}(SO(2))$ and we set $(\pi_1, \pi_2, \pi_3) = (2/3, 1/6, 1/6)$. We then generate a simulation truth and hypothetical data by the following steps:

1. We sample $v_1, v_2, v_3 \stackrel{i.i.d.}{\sim} \mathcal{U}(\mathbb{S})$, $\mu_1, \mu_2, \mu_3 \stackrel{i.i.d.}{\sim} \mathcal{N}(0, 9)$, and $\sigma_1^2, \sigma_2^2, \sigma_3^2 \stackrel{i.i.d.}{\sim} IG(3, 1)$.
2. We define predictors $F_1 = f_{v_1} \# \mathcal{N}(\mu_1, \sigma_1^2)$, $F_2 = f_{v_2} \# \mathcal{N}(\mu_2, \sigma_2^2)$, $F_3 = f_{v_3} \# \mathcal{N}(\mu_3, \sigma_3^2)$ where $f_v(x) = vx$, namely, predictors are univariate Gaussians lifted to 2 dimensions. We then define $\hat{F}_1, \hat{F}_2, \hat{F}_3$ to be empirical distributions over 100 i.i.d samples of F_1, F_2, F_3 respectively.
3. We define $\tilde{G} = \text{SWB}_2(f_{A_1} \# F_1, f_{A_2} \# F_2, f_{A_3} \# F_3, \pi_1, \pi_2, \pi_3)$ where $f_A(x) = Ax$, and define the response $G = \tilde{G} * \mathcal{N}(0, 0.01)$. Since G is intractable, we obtain an empirical version of G : $\hat{G} = \text{SWB}_2(f_{A_1} \# \hat{F}_1, f_{A_2} \# \hat{F}_2, f_{A_3} \# \hat{F}_3, \pi_1, \pi_2, \pi_3) * \mathcal{N}(0, 0.01I_2)$ where the SWB is approximated with 100 atoms as discussed in Section 3.3.

Steps 1-3 generate one observation $(\hat{F}_{i,1}, \dots, \hat{F}_{i,K}, \hat{G}_\ell)$. We repeat the process 70 times to obtain a dataset. We select 70% of samples for the training set $\mathcal{S} = \{(\hat{F}_{11}, \hat{F}_{12}, \hat{F}_{13}), \dots, (\hat{F}_{N1}, \hat{F}_{N2}, \hat{F}_{N3})\}$ (with $N = 49$) and the other 30% of samples for the testing set. We compare MMDR with DDR (Nguyen, Ni & Mueller 2025);

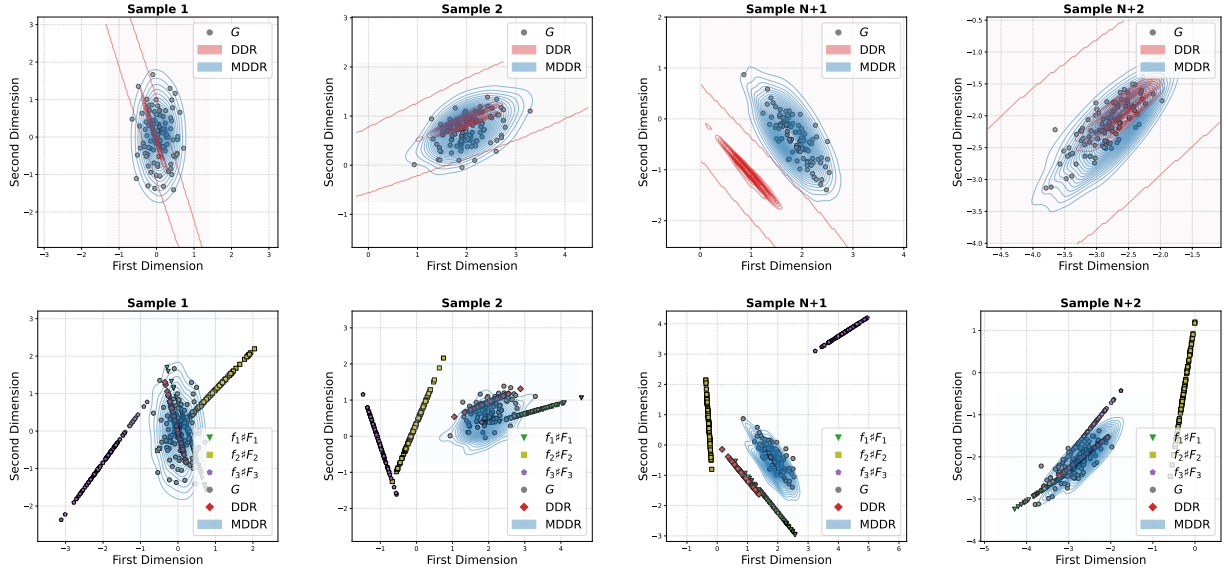


Figure 1: The first two columns display two randomly selected in-sample regression examples ($i = 1, 2$), and the last two columns show two randomly selected out-of-sample examples ($i = N + 1, N + 2$). The first row presents the observed responses G_i , along with the posterior mean fitted distributions $\mathbb{E}(\tilde{G}_i | \text{data})$ for DDR and MDDR.

The second row shows the observed responses, the fitted distributions \tilde{G}_i for DDR and MDDR under the final posterior sample of the chain, and the push-forward $f_{\phi_k} \# \hat{F}_\ell$ of the predictors based on that final posterior sample.

for the latter, we use a linear regression function to regress the response on the first predictor since it does not allow multiple predictors. For both models, we use $w = 10$ for the generalized likelihood and obtain 100 Markov chain samples using MALA, discussed in Section 3.4, with step sizes $\eta_1 = 0.001$ and $\eta_2 = 0.005$. SW distances are approximated using 1000 Monte Carlo projections. For computing SWB, we use $T = 100$, $\eta = 0.1$, and $(\beta_1, \beta_2) = (0.9, 0.999)$.

We report the RE (8) for the training set, the RE for the testing set, and their associated 95% highest credible intervals (HCIs) in Table 1. From the table, we observe that MMDR performs significantly better than DDR in both in-sample fitting and out-of-sample prediction, as expected. An illustration of the results is provided in Figure 1. From the first row of the figure, we see that MMDR yields more accurate posterior means in both the in-sample and out-of-sample settings. We show the posterior mean $\mathbb{E}(\tilde{G}_i | F_i, \text{data})$ of fitted distributions (for display purposes we actually show kernel density estimates (KDE)). MDDR provides

consistently better fits than DDR. The second row of the figure explains why MMDR outperforms DDR: it shows \tilde{G}_i and $f_k \# \hat{F}_{i,k}$ from the last posterior sample in the Markov chain. With a linear regression function, DDR can only produce fitted distributions with a univariate structure. In contrast, MMDR can still provide accurate fitted distributions by leveraging barycenters, although the push-forwards of the predictors also have univariate structures.

Another inference target of interest is the barycenter weights, which indicate the contribution of each predictor to the response. The weights allow us to quantify the strength of association between the predictors and the response. The posterior mean of the barycenter weights is $\bar{\pi} = (0.6482, 0.1808, 0.1710)$, with corresponding 95% posterior credible intervals of $(0.56, 0.1235, 0.1221) - (0.7677, 0.2629, 0.2171)$. The posterior places substantial mass near the true weights $\pi = (2/3, 1/6, 1/6)$. In the next section, we will discuss how to use the posterior of π to construct a cell-cell communication network for single-cell data.

5 Cell-Cell Communication

Cell-cell communication is central to understanding complex biological systems. Interactions between cells underlie a wide range of physiological and pathological processes. A natural approach to quantifying such interactions is to model how the distribution of ligand gene expression of one cell type affects the distribution of receptor gene expressions of another cell type. We showcase the utility of the proposed MDDR framework by applying it to infer communication between a set of cell-types as the senders and a cell-type as the receiver using the population-scale single-cell dataset OneK1K ([Yazar et al. 2022](#)).

We focus on four major cell types: B cells, T cells, monocytes, and NK (natural killer) cells, and set up four regression tasks: (1) Predictors: monocytes, NK cells, and B cells; Response: T cells. (2) Predictors: T cells, monocytes, and NK cells; Response: B cells. (3)

Predictors	Ligands	Response	Receptors
Monocytes	CD86, ICOSL, IL-23, TNF- α , IL-1 β , IL-6, CD70	T Cells	CD3D, CD3E, CD3G, TRBC1, TRBC2, CD28, ICOS, IL-2R, IFNGR, IL-21R, PD-1, CTLA-4, CXCR5, CCR7, CXCR3, CXCR4, IL-12R, IL-15R, IFN- γ R, Tim-3
	IL-15, IFN- γ , CD40L, FasL		
	CD40, CD86, ICOSL, IL-6, BAFF, APRIL		
T Cells	CD40L, IFN- γ	B Cells	IGHM, IGHD, IGHG, IGH α , CD40, ICOSL, IL-21R, IL-6R, BAFFR, CXCR5, CCR7, IL-10R, CXCR4, PD-1, IL-2R, IL-15R, IFN- γ R, CCR1, CXCR2, ICOS, Tim-3
	CD40L, IL-6, TNF- α , Tim-3, BAFF, APRIL		
	IL-15, IFN- γ , CXCL8, CD40L		
B Cells	IL-6, BAFF, TNF- α , CD40L	NK Cells	IL-6R, BAFF-R, TNFR, IL-10R, CCR1, CXCR3, CD40, ICOS, PD-1, Tim-3, NKG2D, IL-2R, IL-4R, IL-21R, IFN- γ R, CD28, NKp30, NKp46, DNAM-1, NKG2A, IL-15R
	IFN- γ , CD86		
	CD40L, TNF- α , IL-15, IL-18, Tim-3		
NK Cells	IL-15, IFN- γ , FasL	Monocytes	IL-12R, IL-15R, IFN- γ R, CXCR3, Fas, CD40, PD-1, Tim-3, CD86, TNFR1, TNFR2, LAG-3, IL-6R, CXCR4
	CD40L, CD70, IL-6, TNF- α , Tim-3, BAFF, APRIL		
	CD40L, IFN- γ , CD70		

Table 2: List of ligands’ genes and receptors’ genes for 4 regression problems (1) Predictors: Monocytes, NK Cells, B Cells, Response: T Cells; (2) Predictors: T Cells, Monocytes, NK Cells, Response: B Cells; (3) Predictors: B Cells, T Cells, Monocytes, Response: NK Cells; (4) Predictors: NK Cells, B Cells, T Cells, Response: Monocytes.

Predictors: B cells, T cells, and monocytes; Response: NK cells. (4) Predictors: NK cells, B cells, and T cells; Response: monocytes. We summarize the list of ligands’ genes and receptors’ genes for all 4 relations in Table 2. From the table, we can see that the number of ligands (the dimension of the predictors) is smaller than the number of receptors (the dimension of the responses), which is similar to our simulation setup in Section 4. We select donors who have at least 90 cells per cell type, which results in 75 donors, and randomly assign 70% of them to the training set and 30% to the testing set.

We again compare the proposed MDDR with DDR, using linear regression functions in both models. Since DDR can only handle one predictor, we set up three separate DDR regression problems for each response variable, each with a different predictor. In both

Response	Model	Train RE	Train RE 95% HCI	Test RE	Test RE 95% HPD
T Cells	DDR (B Cells)	0.2515	0.2482-0.2574	0.2594	0.2533-0.2639
	DDR (Monocytes)	0.3552	0.3522-0.3587	0.3644	0.3565-0.3710
	DDR (NK Cells)	0.5085	0.5060-0.5113	0.5195	0.5164-0.5242
	MDDR	0.1945	0.182-0.2174	0.2021	0.1879-0.2293
B Cells	DDR (T Cells)	0.6131	0.6072-0.6175	0.6083	0.6011-0.6177
	DDR (Monocytes)	0.4515	0.4447-0.4576	0.4619	0.4552-0.4689
	DDR (NK Cells)	0.6210	0.6165-0.6256	0.6630	0.6512-0.669
	MDDR	0.3685	0.3419-0.4076	0.379	0.3478-0.423
Monocytes	DDR (T Cells)	0.5554	0.5422-0.5662	0.5275	0.5150-0.5389
	DDR (B Cells)	0.3844	0.3783-0.3905	0.4080	0.3974-0.4198
	DDR (NK Cells)	0.5629	0.5486-0.5716	0.5496	0.5380-0.5587
	MDDR	0.3142	0.2749-0.3845	0.3162	0.2761-0.4023
NK Cells	DDR (T Cells)	0.8000	0.7951-0.8066	0.7587	0.7518-0.7648
	DDR (B Cells)	0.4786	0.4734-0.4848	0.4959	0.4893-0.5021
	DDR (Monocytes)	0.4661	0.4625-0.4699	0.4537	0.4470-0.4615
	MDDR	0.3604	0.3333-0.3817	0.3625	0.3401-0.3906

Table 3: Average residual errors (RE) for single-predictor DDR models and the multi-predictor MDDR model across four cell types. Reported are training and test relative errors (RE) with their 95% highest posterior density (HPD) intervals.

methods, we set $w = 100$ for the generalized likelihood and draw 100 posterior samples using the MALA, described in Section 3.4, with step sizes $\eta_1 = 0.001$ and $\eta_2 = 0.005$. SW distances are approximated using 100 Monte Carlo projections during inference and are approximated using 1000 Monte Carlo projections during evaluation (RE computation). For computing SWB, we set $T = 100$, $\eta = 0.1$, and $(\beta_1, \beta_2) = (0.9, 0.999)$.

Table 3 summarizes residual errors under MDDR compared with single-predictor DDR models across all four response types. In every setting, MDDR achieves the lowest RE on both the training and test sets, with substantially narrower or comparable 95% HCI ranges, demonstrating improvements in estimation stability and generalization. The results echo similar experience with simple versus multiple (normal linear) regression, and underscore the advantage of jointly modeling multiple predictors. MDDR more effectively captures cross-cell-type relationships than any DDR model based on a single predictor, particularly when the response has higher dimensionality than the predictors.

We show the observed responses and the posterior means of fitted DDR and MDDR

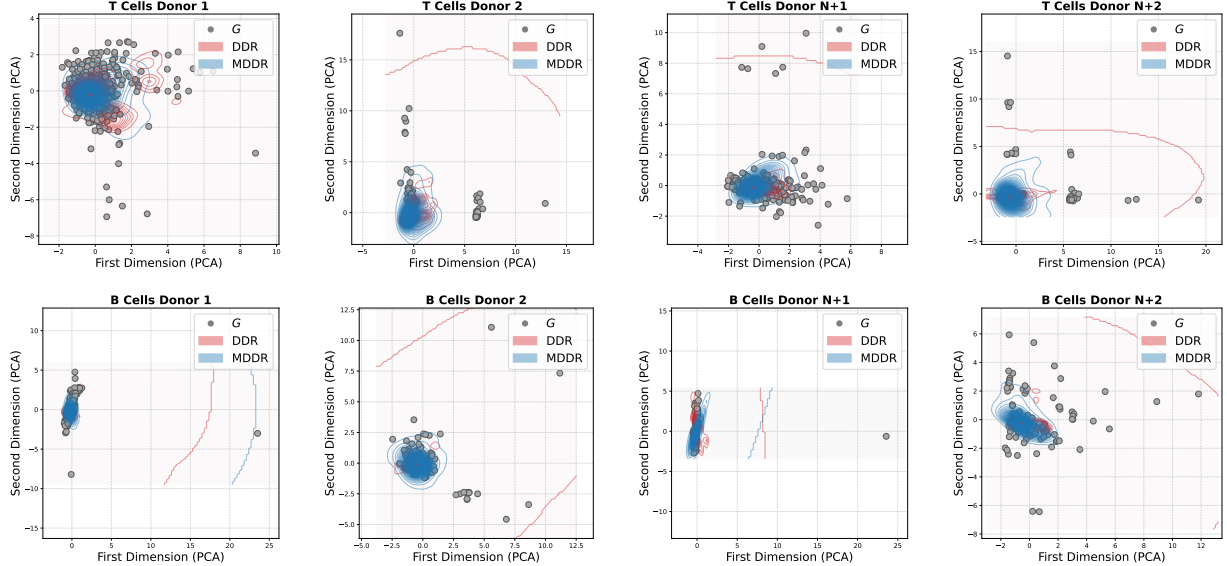


Figure 2: The first two columns show two random in-sample donors and the last two columns show two random out-sample donors. The first row presents results for T Cells including the observed responses, and the posterior means of the KDEs of fitted distributions of DDR and MDDR. The second row presents similar results for B Cells. We use PCA for visualization.

distributions (again, for display purposes showing KDE’s) for T cells and B cells in Figure 2. MDDR provides noticeably better fits than DDR for both training and testing donors. The fitted distributions from MDDR capture the uncertainty in the observed responses more accurately. While the fit could be further improved by using more expressive regression functions beyond linear models, we believe that linear regression functions, being both parsimonious and computationally efficient, are sufficient in this setting. In Figure 4 of Supplementary Material B, we present analogous results for Monocytes and NK cells with the same conclusion: MDDR consistently outperforms DDR. Overall, these qualitative observations align well with the quantitative summaries in Table 3.

Lastly, we highlight an important feature of inference under the proposed MMDR model: it naturally induces a graph structure between predictors and the response (cell types in this case). From (6) and (7), MDDR constructs the fitted distribution as a barycenter of the push-forwards of the predictors. The barycenter weights determine how much each predictor contributes to the resulting fitted distribution. Because these weights lie on a simplex, they

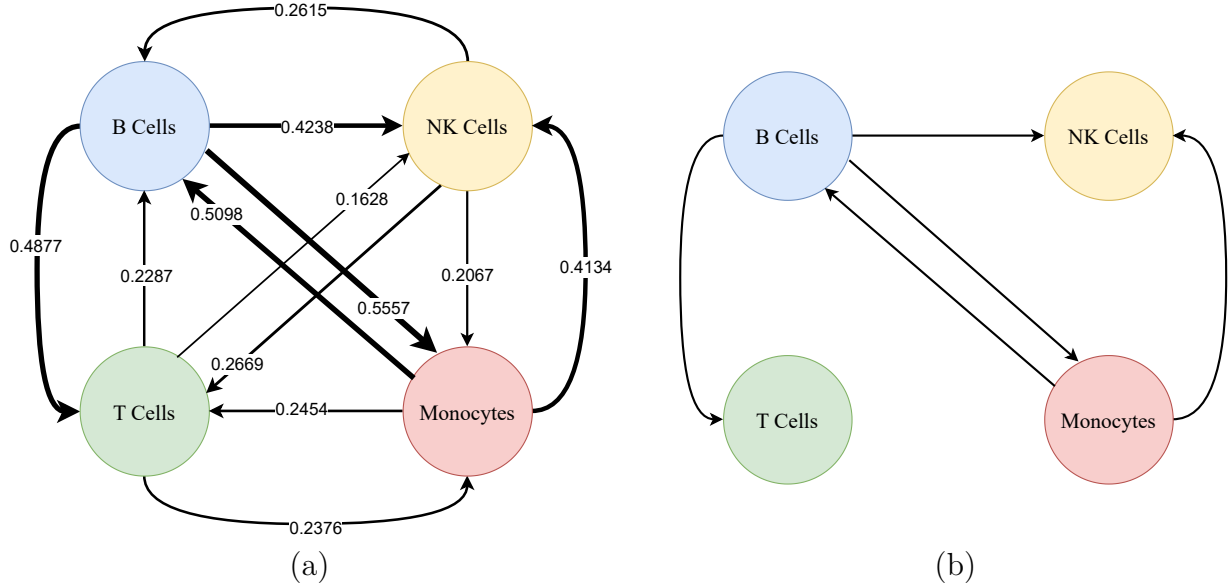


Figure 3: (a) Weighted graph using posterior means of the barycenter weights (weights of edges) under the MMDR model. (b) Sparse graph obtained from the weighted graph by retaining only the edges whose weights exceed $1/3$.

can be interpreted as degrees of association (ranging from 0 to 1) between predictors and the response. Across the four regression problems corresponding to the four cell types, we can construct a weighted graph whose vertices represent the cell types. Each vertex has three incoming edges from the other vertices, corresponding to the associated MDDR problems. We assign each edge the posterior mean of the corresponding barycenter weight. The resulting weighted graph is shown in Figure 3(a). Finally, to enhance interpretability, we drop edges with weights smaller than $1/3$ (the mean of the Dirichlet prior) yielding the sparse graph shown in Figure 3(b). From this graph, we observe evidence that B cells interact with all other cell types, while Monocytes interact only with B cells and NK cells. In contrast, NK cells and T cells do not interact with any other cell types.

6 Conclusion

We introduced Bayesian multiple multivariate density–density regression as a novel framework for modeling complex regression relationships, where a multivariate random distribution

serves as the response and multiple random distributions act as predictors.

Several limitations remain. First, the framework may be sensitive to model misspecification because it relies on parametric regression functions f_ϕ . Nevertheless, in both simulations and real-data applications, we found these mappings to be sufficiently flexible in practice. Second, the approximation of the sliced Wasserstein barycenter (SWB) used in our implementation may not be optimal in terms of computational efficiency or approximation accuracy. For the datasets considered in the paper, however, the current approximation proved adequate.

Future work will aim to address these limitations. For example, the framework could be extended to a Bayesian nonparametric setting for multiple multivariate density–density regression. Additionally, alternative approximation strategies, such as more efficient iterative schemes with improved convergence or deterministic fast approximations of the SWB, could further enhance performance.

References

- Bissiri, P. G., Holmes, C. C. & Walker, S. G. (2016), ‘A general framework for updating belief distributions’, *Journal of the Royal Statistical Society Series B: Statistical Methodology* **78**(5), 1103–1130.
- Boedihardjo, M. T. (2025), ‘Sharp bounds for max-sliced Wasserstein distances’, *Foundations of Computational Mathematics* pp. 1–32.
- Bonneel, N., Rabin, J., Peyré, G. & Pfister, H. (2015), ‘Sliced and Radon Wasserstein barycenters of measures’, *Journal of Mathematical Imaging and Vision* **1**(51), 22–45.
- Chen, X., Fu, M., Huang, Y. & Deng, X. (2024), ‘Distribution-in-distribution-out regression’, *arXiv preprint arXiv:2405.11626* .
- Cuturi, M. & Doucet, A. (2014), Fast computation of Wasserstein barycenters, in ‘International conference on machine learning’, PMLR, pp. 685–693.
- Dunson, D. B., Pillai, N. & Park, J.-H. (2007), ‘Bayesian density regression’, *Journal of the Royal Statistical Society Series B: Statistical Methodology* **69**(2), 163–183.
- Fournier, N. & Guillin, A. (2015), ‘On the rate of convergence in Wasserstein distance of the empirical measure’, *Probability theory and related fields* **162**(3), 707–738.
- Girolami, M. & Calderhead, B. (2011), ‘Riemann manifold Langevin and Hamiltonian Monte Carlo methods’, *Journal of the Royal Statistical Society Series B: Statistical Methodology* **73**(2), 123–214.
- Goldfeld, Z., Kato, K., Rioux, G. & Sadhu, R. (2024), ‘Statistical inference with regularized optimal transport’, *Information and Inference: A Journal of the IMA* **13**(1), iaad056.
- Kingma, D. P. & Ba, J. (2014), ‘Adam: A method for stochastic optimization’, *arXiv preprint arXiv:1412.6980* .

Manole, T., Balakrishnan, S. & Wasserman, L. (2022), ‘Minimax confidence intervals for the sliced Wasserstein distance’, *Electronic Journal of Statistics* **16**(1), 2252–2345.

Matabuena, M. & Petersen, A. (2023), ‘Distributional data analysis of accelerometer data from the NHANES database using nonparametric survey regression models’, *Journal of the Royal Statistical Society Series C: Applied Statistics* **72**(2), 294–313.

Nadjahi, K., Durmus, A., Chizat, L., Kolouri, S., Shahrampour, S. & Simsekli, U. (2020), ‘Statistical and topological properties of sliced probability divergences’, *Advances in Neural Information Processing Systems* **33**, 20802–20812.

Nguyen, K. (2025), ‘An introduction to sliced optimal transport: Foundations, advances, extensions, and applications’, *Foundations and Trends® in Computer Graphics and Vision* **17**(3-4), 171–406.

URL: <http://dx.doi.org/10.1561/0600000119>

Nguyen, K., Ho, N., Pham, T. & Bui, H. (2021), Distributional sliced-Wasserstein and applications to generative modeling, in ‘International Conference on Learning Representations’.

URL: <https://openreview.net/forum?id=QYjO70ACDK>

Nguyen, K., Nguyen, H. & Ho, N. (2025), Towards marginal fairness sliced Wasserstein barycenter, in ‘The Thirteenth International Conference on Learning Representations’.

URL: <https://openreview.net/forum?id=NQqJPPCesd>

Nguyen, K., Ni, Y. & Mueller, P. (2025), ‘Bayesian multivariate density-density regression’, *arXiv preprint arXiv:2504.12617*.

Nietert, S., Goldfeld, Z., Sadhu, R. & Kato, K. (2022), ‘Statistical, robustness, and computational guarantees for sliced Wasserstein distances’, *Advances in Neural Information Processing Systems* **35**, 28179–28193.

Ning, N. (2025), ‘Metropolis-adjusted subdifferential Langevin algorithm’, *arXiv preprint arXiv:2507.06950* .

Park, J., Roy, A., Siegel, J. W. & Bhattacharya, A. (2025), ‘Acceleration via silver step-size on Riemannian manifolds with applications to Wasserstein space’, *Advances in Neural Information Processing System* .

Peyré, G. & Cuturi, M. (2019), ‘Computational optimal transport: With applications to data science’, *Foundations and Trends in Machine Learning* **11**(5-6), 355–607.

Peyré, G., Cuturi, M. et al. (2019), ‘Computational optimal transport: With applications to data science’, *Foundations and Trends in Machine Learning* **11**(5-6), 355–607.

Rabin, J., Peyré, G., Delon, J. & Bernot, M. (2012), Wasserstein barycenter and its application to texture mixing, in ‘Scale Space and Variational Methods in Computer Vision: Third International Conference, SSVM 2011, Ein-Gedi, Israel, May 29–June 2, 2011, Revised Selected Papers 3’, Springer, pp. 435–446.

Shen, W. & Ghosal, S. (2016), ‘Adaptive Bayesian density regression for high-dimensional data’, *Bernoulli* pp. 396–420.

Szabó, Z., Sriperumbudur, B. K., Póczos, B. & Gretton, A. (2016), ‘Learning theory for distribution regression’, *Journal of Machine Learning Research* **17**(152), 1–40.

Tokdar, S. T., Zhu, Y. M. & Ghosh, J. K. (2004), ‘Bayesian density regression with logistic Gaussian process and subspace projection’, *Bayesian Analysis* **1**(1).

Villani, C. (2009), *Optimal transport: old and new*, Vol. 338, Springer.

Wilson, A. G. & Izmailov, P. (2020), ‘Bayesian deep learning and a probabilistic perspective of generalization’, *Advances in neural information processing systems* **33**, 4697–4708.

Yazar, S., Alquicira-Hernandez, J., Wing, K., Senabouth, A., Gordon, M. G., Andersen,

S., Lu, Q., Rowson, A., Taylor, T. R., Clarke, L. et al. (2022), ‘Single-cell eQTL mapping identifies cell type-specific genetic control of autoimmune disease’, *Science* **376**(6589), eabf3041.

Zhao, Y., Datta, A., Tang, B., Zipunnikov, V. & Caffo, B. S. (2023), ‘Density-on-density regression’, *arXiv preprint arXiv:2307.03642* .

Zhu, C. & Müller, H.-G. (2023), ‘Geodesic optimal transport regression’, *arXiv preprint arXiv:2312.15376* .

Supplementary Materials for “Bayesian Multiple Multivariate
Density-Density Regression”

A Proofs

A.1 Proof of Lemma 1

We first state a lemma on a projection of SWB. In particular, we show that a projection of SWB is a Wasserstein barycenter of corresponding projected marginals.

Lemma 2 (Projection of sliced Wasserstein barycenter). *Let $F_1, \dots, F_K \in \mathcal{P}_p(\mathbb{R})$ with weights $(\pi_1, \dots, \pi_K) \in \Delta$, $\bar{F} = SWB_p(F_1, \dots, F_K, \pi_1, \dots, \pi_K)$. Then for almost every $\theta \in \mathbb{S}^{d-1}$, the projection $\theta \sharp \bar{F}$ of \bar{F} along θ*

$$\theta \sharp \bar{F} = WB_p(\theta \sharp F_1, \dots, \theta \sharp F_K, \pi_1, \dots, \pi_K), \quad (39)$$

is the 1D Wasserstein barycenter of the projected measures $\theta \sharp F_k$.

Proof. The objective of the defining optimization problem for SW barycenter can be written as:

$$\mathcal{L}(\bar{F}) = \int_{\theta \in \mathbb{S}^{d-1}} L_\theta(\theta \sharp \bar{F}) d\sigma(\theta), \text{ where } L_\theta(\theta \sharp \bar{F}) := \sum_{k=1}^K \pi_k W_p^p(\theta \sharp \bar{F}, \theta \sharp F_k), \quad (40)$$

and $\sigma(\theta)$ is the uniform measure on \mathbb{S}^{d-1} . Since the integrand $L(\theta \sharp \bar{F})$ is nonnegative, the integral is minimized if and only if for almost every θ ,

$$\theta \sharp \bar{F} = \arg \min_{\nu \in \mathcal{P}_2(\mathbb{R})} L_\theta(\nu) = WB_p(\theta \sharp F_1, \dots, \theta \sharp F_K, \pi_1, \dots, \pi_K). \quad (41)$$

Otherwise, one could replace the projection along any positive-measure set of θ by its 1D minimizer, decreasing the integral and contradicting the minimality of \bar{F} .

□

(a) By the definition of SW and Lemma 2 and the fact that $Q_{\theta \sharp \bar{F}} = \sum_{k=1}^K \pi_k Q_{\theta \sharp F_k}$ (Bonneel et al. 2015), we have

$$\begin{aligned}
\text{SW}_p^p(\bar{F}, \bar{F}') &= \mathbb{E}_{\theta \sim \mathcal{U}(\mathbb{S}^{d-1})} [W_p^p(\theta \sharp \bar{F}, \theta \sharp \bar{F}')] \\
&= \mathbb{E}_{\theta \sim \mathcal{U}(\mathbb{S}^{d-1})} \left[\int_0^1 |Q_{\theta \sharp \bar{F}}(t) - Q_{\theta \sharp \bar{F}'}(t)|^p dt \right] \\
&= \mathbb{E}_{\theta \sim \mathcal{U}(\mathbb{S}^{d-1})} \left[\int_0^1 \left| \sum_{k=1}^K \pi_k Q_{\theta \sharp F_k}(t) - \sum_{k=1}^K \pi_k Q_{\theta \sharp F'_k}(t) \right|^p dt \right] \\
&\leq \mathbb{E}_{\theta \sim \mathcal{U}(\mathbb{S}^{d-1})} \left[\int_0^1 \sum_{k=1}^K \pi_k |Q_{\theta \sharp F_k}(t) - Q_{\theta \sharp F'_k}(t)|^p dt \right] \\
&= \sum_{k=1}^K \pi_k \mathbb{E}_{\theta \sim \mathcal{U}(\mathbb{S}^{d-1})} \left[\int_0^1 |Q_{\theta \sharp F_k}(t) - Q_{\theta \sharp F'_k}(t)|^p dt \right] \\
&= \sum_{k=1}^K \pi_k \text{SW}_p^p(F_k, F'_k), \tag{42}
\end{aligned}$$

where the inequality is due to Jensen's inequality, and the following equality is due to the Fubini's theorem.

(b) Again, by the definition of SW and Lemma 2 and the fact that $Q_{\theta \sharp \bar{F}} = \sum_{k=1}^K \pi_k Q_{\theta \sharp F_k}$ (Bon-

neel et al. 2015), we have

$$\begin{aligned}
\text{SW}_p^p(\bar{F}, \bar{F}') &= \mathbb{E}_{\theta \sim \mathcal{U}(\mathbb{S}^{d-1})} [W_p^p(\theta \sharp \bar{F}, \theta \sharp \bar{F}')] \\
&= \mathbb{E}_{\theta \sim \mathcal{U}(\mathbb{S}^{d-1})} \left[\int_0^1 |Q_{\theta \sharp \bar{F}}(t) - Q_{\theta \sharp \bar{F}'}(t)|^p dt \right] \\
&= \mathbb{E}_{\theta \sim \mathcal{U}(\mathbb{S}^{d-1})} \left[\int_0^1 \left| \sum_{k=1}^K \pi_k Q_{\theta \sharp F_k}(t) - \sum_{k=1}^K \pi'_k Q_{\theta \sharp F'_k}(t) \right|^p dt \right] \\
&\leq \mathbb{E}_{\theta \sim \mathcal{U}(\mathbb{S}^{d-1})} \left[\int_0^1 \left(\left| \sum_{k=1}^K \pi_k (Q_{\theta \sharp F_k}(t) - Q_{\theta \sharp F'_k}(t)) \right| \right. \right. \\
&\quad \left. \left. + \left| \sum_{k=1}^K (\pi'_k - \pi_k) Q_{\theta \sharp F'_k}(t) \right| \right)^p dt \right] \\
&\leq 2^{p-1} \mathbb{E}_{\theta \sim \mathcal{U}(\mathbb{S}^{d-1})} \left[\int_0^1 \left(\left| \sum_{k=1}^K \pi_k (Q_{\theta \sharp F_k}(t) - Q_{\theta \sharp F'_k}(t)) \right| \right)^p dt \right] \\
&\quad + \mathbb{E}_{\theta \sim \mathcal{U}(\mathbb{S}^{d-1})} \left[\int_0^1 \left(\left| \sum_{k=1}^K (\pi'_k - \pi_k) Q_{\theta \sharp F'_k}(t) \right| \right)^p dt \right]. \tag{43}
\end{aligned}$$

From Lemma 1, we know that

$$\begin{aligned}
\mathbb{E}_{\theta \sim \mathcal{U}(\mathbb{S}^{d-1})} \left[\int_0^1 \left(\left| \sum_{k=1}^K \pi_k (Q_{\theta \sharp F_k}(t) - Q_{\theta \sharp F'_k}(t)) \right| \right)^p dt \right] &\leq \sum_{k=1}^K \pi_k \text{SW}_p^p(F_k, F'_k) \\
&\leq \max_{k \in \{1, \dots, K\}} \text{SW}_p^p(F_k, F'_k), \tag{44}
\end{aligned}$$

since $\pi \in \Delta^K$. For the second term, we have

$$\begin{aligned}
&\mathbb{E}_{\theta \sim \mathcal{U}(\mathbb{S}^{d-1})} \left[\int_0^1 \left| \sum_{k=1}^K (\pi'_k - \pi_k) Q_{\theta \sharp F'_k}(t) \right|^p dt \right] \\
&\leq \mathbb{E}_{\theta \sim \mathcal{U}(\mathbb{S}^{d-1})} \left[\int_0^1 \left(\sum_{k=1}^K |\pi'_k - \pi_k| |Q_{\theta \sharp F'_k}(t)| \right)^p dt \right] \\
&\leq \mathbb{E}_{\theta \sim \mathcal{U}(\mathbb{S}^{d-1})} \left[\left(\sum_{k=1}^K |\pi'_k - \pi_k| \left(\int_0^1 |Q_{\theta \sharp F'_k}(t)|^p dt \right)^{1/p} \right)^p \right] \\
&\leq \left(\sum_{k=1}^K |\pi'_k - \pi_k| \left(\mathbb{E}_{\theta \sim \mathcal{U}(\mathbb{S}^{d-1})} \int_0^1 |Q_{\theta \sharp F'_k}(t)|^p dt \right)^{1/p} \right)^p \\
&\leq \|\pi' - \pi\|_p^p M, \tag{45}
\end{aligned}$$

where

$$M = \left(\sum_{k=1}^K \left(\mathbb{E}_{\theta \sim \mathcal{U}(\mathbb{S}^{d-1})} \int_0^1 |Q_{\theta \# F'_k}(t)|^p dt \right)^{1/(p-1)} \right)^{(p-1)},$$

the second inequality is due to Minkowski's inequality, and the third inequality is due to Jensen's inequality. From (43), (44), and (45), we obtain the desired bound and complete the proof.

A.2 Proof of Theorem 1

Using the mean value theorem for the exponential function, we have

$$e^x - e^y = e^c(x - y), \quad (46)$$

for any $x, y \in \mathbb{R}$ and some $c \in [x, y]$. Therefore, we have

$$|e^x - e^y| \leq \max\{e^x, e^y\}|x - y|. \quad (47)$$

Apply the above inequality to our case, we obtain:

$$\begin{aligned} & \mathbb{E} \left[\left| \exp\{-w\text{SW}_p^p(\bar{F}, G)\} - \exp\{-w\text{SW}_p^p(\hat{\bar{F}}, \hat{G})\} \right| \right] \\ & \leq \mathbb{E} \left[\max\{\exp\{-w\text{SW}_p^p(\bar{F}, G)\}, \exp\{-w\text{SW}_p^p(\hat{\bar{F}}, \hat{G})\}\} \left| w(\text{SW}_p^p(\bar{F}, G) - \text{SW}_p^p(\hat{\bar{F}}, \hat{G})) \right| \right] \\ & \leq w\mathbb{E} \left[\left| \text{SW}_p^p(\bar{F}, G) - \text{SW}_p^p(\hat{\bar{F}}, \hat{G}) \right| \right], \end{aligned} \quad (48)$$

where the last inequality is due to the fact that $\text{SW}_p^p(\bar{F}, G) \geq 0$ and $\text{SW}_p^p(\hat{\bar{F}}, \hat{G}) \geq 0$ which implies $\exp(-w\text{SW}_p^p(\bar{F}, G)) \leq 1$ and $\exp(-w\text{SW}_p^p(\hat{\bar{F}}, \hat{G})) \leq 1$. Using Jensen's inequality,

we have:

$$\begin{aligned}
& w\mathbb{E} \left[\left| \exp\{-w\text{SW}_p^p(\bar{F}, G)\} - \exp\{-w\text{SW}_p^p(\hat{\bar{F}}, \hat{G})\} \right| \right] \\
& \leq w\mathbb{E} \left[\left| \text{SW}_p^p(\bar{F}, G) - \text{SW}_p^p(\hat{\bar{F}}, \hat{G}) \right| \right] \\
& = w\mathbb{E} \left[\mathbb{E}_\theta \left[W_p^p(\theta \sharp \bar{F}, \theta \sharp G) - W_p^p(\theta \sharp \hat{\bar{F}}, \theta \sharp \hat{G}) \right] \right] \\
& \leq w\mathbb{E} \left[\mathbb{E}_\theta \left[W_p^p(\theta \sharp \bar{F}, \theta \sharp G) - W_p^p(\theta \sharp \hat{\bar{F}}, \theta \sharp \hat{G}) \right] \right]. \tag{49}
\end{aligned}$$

Using Lemma 4 in [Goldfeld et al. \(2024\)](#) with compact support with diameter $R > 0$, we further have:

$$\begin{aligned}
& \mathbb{E} \left[\mathbb{E}_\theta \left[\left| W_p^p(\theta \sharp \bar{F}, \theta \sharp G) - W_p^p(\theta \sharp \hat{\bar{F}}, \theta \sharp \hat{G}) \right| \right] \right] \\
& \leq C_{p,R} \mathbb{E} \left[\mathbb{E}_\theta \left[\left| W_1(\theta \sharp \bar{F}, \theta \sharp \hat{\bar{F}}) + W_1(\theta \sharp G, \theta \sharp \hat{G}) \right| \right] \right] \\
& = C_{p,R} \mathbb{E} \left[\text{SW}_1(\bar{F}, \hat{\bar{F}}) + \text{SW}_1(G, \hat{G}) \right] \tag{50}
\end{aligned}$$

Using Lemma 1, we further have:

$$\begin{aligned}
& C_{p,R} \mathbb{E} \left[\text{SW}_1(\bar{F}, \hat{\bar{F}}) + \text{SW}_1(G, \hat{G}) \right] \\
& \leq C_{p,R} \mathbb{E} \left[\sum_{k=1}^K \pi_k \text{SW}_1(F_k, \hat{F}_k) + \text{SW}_1(G, \hat{G}) \right] \\
& = C_{p,R} \sum_{k=1}^K \pi_k \mathbb{E} \left[\text{SW}_1(F_k, \hat{F}_k) \right] + \mathbb{E} \left[\text{SW}_1(G, \hat{G}) \right] \tag{51}
\end{aligned}$$

which turns into the sample complexity of SW_1 . The sample complexity of SW_1 has been investigated in [Nadjahi et al. \(2020\)](#), [Nguyen et al. \(2021\)](#), [Manole et al. \(2022\)](#), [Nietert et al. \(2022\)](#), [Boedihardjo \(2025\)](#). We provide a proof based on compact support:

$$\begin{aligned}
\mathbb{E} [\text{SW}_1(G, \hat{G})] &= \mathbb{E} [\mathbb{E}_\theta [W_1(\theta \sharp G, \theta \sharp \hat{G})]] \\
&= \mathbb{E} [\mathbb{E}_\theta \left[\int_{\mathbb{R}} |F_{\theta \sharp G}(x) - F_{\theta \sharp \hat{G}}(x)| dx \right]] \\
&\leq R \mathbb{E} [\mathbb{E}_\theta \left[\sup_x |F_{\theta \sharp G}(x) - F_{\theta \sharp \hat{G}}(x)| \right]] \\
&= R \mathbb{E}_\theta \left[\mathbb{E} \left[\sup_x |F_{\theta \sharp G}(x) - F_{\theta \sharp \hat{G}}(x)| \right] \right], \tag{52}
\end{aligned}$$

by Fubini's theorem. From Dvoretzky–Kiefer–Wolfowitz's inequality, we know that

$$\mathbb{P}(\sup_x |F_{\theta \sharp G}(x) - F_{\theta \sharp \hat{G}}(x)| > \epsilon) \leq 2 \exp(-2n\epsilon^2), \tag{53}$$

for any $\epsilon > 0$ and $\theta \in \mathbb{S}^{d-1}$. Therefore,

$$\begin{aligned}
\mathbb{E} \left[\sup_x |F_{\theta \sharp G}(x) - F_{\theta \sharp \hat{G}}(x)| \right] &= \int_0^\infty \mathbb{P}(\sup_x |F_{\theta \sharp G}(x) - F_{\theta \sharp \hat{G}}(x)| > \epsilon) d\epsilon \\
&\leq \int_0^\infty 2 \exp(-2n\epsilon^2) d\epsilon \\
&= \sqrt{\frac{\pi}{2n}}, \tag{54}
\end{aligned}$$

due to the Gaussian integral. By Fubini's theorem,

$$\mathbb{E}_\theta \left[\mathbb{E} \left[\sup_x |F_{\theta \sharp G}(x) - F_{\theta \sharp \hat{G}}(x)| \right] \right] \leq \sqrt{\frac{\pi}{2n}} \tag{55}$$

From (48), (50), (51), (52), and (55), we obtain

$$\mathbb{E} \left[\left| \exp(-w \text{SW}_p^p(\bar{F}, G)) - \exp(-w \text{SW}_p^p(\hat{F}, \hat{G})) \right| \right] \leq C_{p,R,w} \frac{1}{\sqrt{n}}, \tag{56}$$

for a constant $C_{p,R,w}$ depends on p, w, R , which completes the proof.

A.3 Proof of Theorem 2

We first establish a modulus continuity for $|\text{SW}_p^p(\tilde{G}(\phi, \pi), G) - \text{SW}_p^p(\tilde{G}(\phi', \pi'), G)|$, which is later used for proving uniform law of large numbers for the empirical risk.

Lemma 3. *Under Assumptions 3 and 5, we have*

$$|\text{SW}_p^p(\tilde{G}(\phi, \pi), G) - \text{SW}_p^p(\tilde{G}(\phi', \pi'), G)| \leq \gamma(\|\phi - \phi'\|_p^p + \|\pi - \pi'\|_p^p), \quad (57)$$

for a modulus of continuity $\gamma : \mathbb{R}_+ \rightarrow \mathbb{R}_+$ such that $\lim_{t \rightarrow 0} \gamma(t) = 0$.

Proof. Using the inequality $|a^p - b^p| \leq p \max\{a^{p-1}, b^{p-1}\}|a - b|$, we have

$$\begin{aligned} & |\text{SW}_p^p(\tilde{G}(\phi, \pi), G) - \text{SW}_p^p(\tilde{G}(\phi', \pi'), G)| \\ & \leq p \max\{\text{SW}_p(\tilde{G}(\phi, \pi), G)^{p-1}, \text{SW}_p(\tilde{G}(\phi', \pi'), G)^{p-1}\} \\ & \quad |\text{SW}_p(\tilde{G}(\phi, \pi), G) - \text{SW}_p(\tilde{G}(\phi', \pi'), G)|. \end{aligned} \quad (58)$$

We first bound the difference $|\text{SW}_p(\tilde{G}(\phi, \pi), G) - \text{SW}_p(\tilde{G}(\phi', \pi'), G)|$ for $\phi, \phi' \in \Phi$. Using the triangle inequality of SW_p , we have:

$$\begin{aligned} & |\text{SW}_p(\tilde{G}(\phi, \pi), G) - \text{SW}_p(\tilde{G}(\phi', \pi'), G)| \\ & \leq |\text{SW}_p(\tilde{G}(\phi, \pi), \tilde{G}(\phi', \pi')) + \text{SW}_p(\tilde{G}(\phi', \pi'), G) - \text{SW}_p(\tilde{G}(\phi', \pi'), G)| \\ & = \text{SW}_p(\tilde{G}(\phi, \pi), \tilde{G}(\phi', \pi')) \\ & \leq \left(2^{p-1} \max_{k \in \{1, \dots, K\}} \text{SW}_p^p(f_{k, \phi_k} \# F_k, f_{k, \phi'_k} \# F_k) + M \|\pi - \pi'\|_p^p\right)^{\frac{1}{p}}, \end{aligned} \quad (59)$$

where the last inequality is due to Lemma 1 (b). We further have:

$$\begin{aligned}
& \text{SW}_p^p(f_{k,\phi_k} \# F_k, f_{k,\phi'_k} \# F_k) \\
&= \mathbb{E}_{\theta \sim \mathcal{U}(\mathbb{S}^{d-1})} [W_p^p(\theta \# f_{k,\phi_k} \# F_k, \theta \# f_{k,\phi'_k} \# F_k)] \\
&= \mathbb{E}_{\theta \sim \mathcal{U}(\mathbb{S}^{d-1})} \left[\inf_{\pi \in \Pi(F_k, F_k)} \mathbb{E}_{(X,Y) \sim \pi} [|\theta^\top f_{k,\phi_k}(X) - \theta^\top f_{k,\phi'_k}(Y)|^p] \right] \\
&\leq \mathbb{E}_{\theta \sim \mathcal{U}(\mathbb{S}^{d-1})} \left[\mathbb{E}_{(X,Y) \sim (Id, Id) \# F_k} [|\theta^\top f_{k,\phi_k}(X) - \theta^\top f_{k,\phi'_k}(Y)|^p] \right] \\
&= \mathbb{E}_{\theta \sim \mathcal{U}(\mathbb{S}^{d-1})} \left[\mathbb{E}_{X \sim F_k} [|\theta^\top f_{k,\phi_k}(X) - \theta^\top f_{k,\phi'_k}(X)|^p] \right] \\
&\leq \mathbb{E}_{\theta \sim \mathcal{U}(\mathbb{S}^{d-1})} \left[\mathbb{E}_{X \sim F_k} [\|f_{k,\phi_k}(X) - f_{k,\phi'_k}(X)\|_p^p] \right] \\
&= \mathbb{E}_{X \sim F_k} [\|f_{k,\phi_k}(X) - f_{k,\phi'_k}(X)\|_p^p] \leq \omega_k (\|\phi_k - \phi'_k\|_p^p), \tag{60}
\end{aligned}$$

where the second inequality is due to the Cauchy–Schwarz’s inequality and $\|\theta\|_2^2 = 1$, and

the last inequality is due to Assumption 5. Therefore, we have:

$$\begin{aligned}
& |\text{SW}_p(\tilde{G}(\phi, \pi), G) - \text{SW}_p(\tilde{G}(\phi', \pi'), G)| \\
&\leq \left(2^{p-1} \max_{k \in \{1, \dots, K\}} \omega_k (\|\phi_k - \phi'_k\|_p^p) + M \|\pi - \pi'\|_p^p \right)^{\frac{1}{p}} \\
&\leq \left(2^{p-1} \max_{k \in \{1, \dots, K\}} \omega_k (\|\phi - \phi'\|_p^p) + M \|\pi - \pi'\|_p^p \right)^{\frac{1}{p}} \\
&\leq \left(2^{p-1} \max_{k \in \{1, \dots, K\}} \omega_k (\|\phi - \phi'\|_p^p + \|\pi - \pi'\|_p^p) + M (\|\phi - \phi'\|_p^p + \|\pi - \pi'\|_p^p) \right)^{\frac{1}{p}}
\end{aligned}$$

where $\|\phi - \phi'\|_p^p = \sum_{k=1}^K \|\phi_k - \phi'_k\|_p^p$.

We now bound $\max\{\text{SW}_p(\tilde{G}(\phi, \pi), G)^{p-1}, \text{SW}_p(\tilde{G}(\phi', \pi'), G)^{p-1}\}$. We have

$$\begin{aligned}
\text{SW}_p^p(\tilde{G}(\phi, \pi), G) &= \mathbb{E}_{\theta \sim \mathcal{U}(\mathbb{S}^{d-1})} \left[\int_0^1 |Q_{\theta \sharp \tilde{G}(\phi, \pi)}(t) - Q_{\theta \sharp G}(t)|^p dt \right] \\
&= \mathbb{E}_{\theta \sim \mathcal{U}(\mathbb{S}^{d-1})} \left[\int_0^1 \left| \sum_{k=1}^K \pi_k Q_{\theta \sharp f_k, \phi_k \sharp F_k}(t) - Q_{\theta \sharp G}(t) \right|^p dt \right] \\
&= \mathbb{E}_{\theta \sim \mathcal{U}(\mathbb{S}^{d-1})} \left[\int_0^1 \left| \sum_{k=1}^K \pi_k Q_{\theta \sharp f_k, \phi_k \sharp F_k}(t) - Q_{\theta \sharp G}(t) \right|^p dt \right] \\
&\leq \mathbb{E}_{\theta \sim \mathcal{U}(\mathbb{S}^{d-1})} \left[\int_0^1 \sum_{k=1}^K \pi_k \left| Q_{\theta \sharp f_k, \phi_k \sharp F_k}(t) - Q_{\theta \sharp G}(t) \right|^p dt \right] \\
&= \sum_{k=1}^K \pi_k \mathbb{E}_{\theta \sim \mathcal{U}(\mathbb{S}^{d-1})} \left[\int_0^1 \left| Q_{\theta \sharp f_k, \phi_k \sharp F_k}(t) - Q_{\theta \sharp G}(t) \right|^p dt \right] \\
&= \sum_{k=1}^K \pi_k \text{SW}_p^p(f_k, \phi_k \sharp F_k, G) \\
&\leq \max_{k \in \{1, \dots, K\}} \text{SW}_p^p(f_k, \phi_k \sharp F_k, G) \\
&= \max_{k \in \{1, \dots, K\}} \mathbb{E}_{\theta \sim \mathcal{U}(\mathbb{S}^{d-1})} \left[\inf_{\pi \in \Pi(F_k, G)} \mathbb{E}_{(X, Y) \sim \pi} [\|\theta^\top f_k, \phi_k(X) - \theta^\top Y\|_p^p] \right] \\
&\leq \max_{k \in \{1, \dots, K\}} \mathbb{E}_{(X, Y) \sim \pi} [\|f_k, \phi_k(X)\|_p^p + \|Y\|_p^p] \\
&\leq C + C_G. \tag{61}
\end{aligned}$$

With similar reasoning $\text{SW}_p(\tilde{G}(\phi', \pi'), G)$, we have

$$\max\{\text{SW}_p(\tilde{G}(\phi, \pi), G)^{p-1}, \text{SW}_p(\tilde{G}(\phi', \pi'), G)^{p-1}\} \leq (C + C_G)^{(p-1)/p}. \tag{62}$$

As a result, we have

$$\begin{aligned}
& |\text{SW}_p^p(\tilde{G}(\phi, \pi), G) - \text{SW}_p^p(\tilde{G}(\phi', \pi'), G)| \\
& \leq p(C + C_G)^{(p-1)/p} \\
& \quad \left(\max_{k \in \{1, \dots, K\}} \omega_k(\|\phi - \phi'\|_p^p + \|\pi - \pi'\|_p^p) + M(\|\phi - \phi'\|_p^p + \|\pi - \pi'\|_p^p) \right)^{\frac{1}{p}} \\
& = \gamma(\|\phi - \phi'\|_p^p + \|\pi - \pi'\|_p^p), \tag{63}
\end{aligned}$$

where $\gamma(t) = p(C + C_G)^{(p-1)/p} \left(\max_{k \in \{1, \dots, K\}} \omega_k(t) + Mt \right)^{\frac{1}{p}}$ which satisfies $\lim_{t \rightarrow 0} \gamma(t) = 0$.

We conclude the proof here. \square

Lemma 4 (Uniform Law of Large Numbers). *Under assumptions 2, 3, and 5,*

$$\sup_{(\phi, \pi) \in \Phi \times \Delta^K} |R_N(\phi, \pi) - R(\phi, \pi)| \xrightarrow{a.s.} 0 \quad \text{as } N \rightarrow \infty. \tag{64}$$

Proof. Since Φ is compact by Assumption 2 and the simplex Δ^K is already compact, there exists a δ -net $\{(\phi^{(1)}, \pi^{(1)}), \dots, (\phi^{(H)}, \pi^{(H)})\} \subset \Phi \times \Delta^K$ such that for any $(\phi, \pi) \in \Phi \times \Delta^K$, there exists $(\phi^{(h)}, \pi^{(h)}) \in \{(\phi^{(1)}, \pi^{(1)}), \dots, (\phi^{(H)}, \pi^{(H)})\}$ with

$$\|\phi - \phi^{(h)}\|_p^p + \|\pi - \pi^{(h)}\|_p^p \leq \delta. \tag{65}$$

Using Lemma 3, we have for each $i = 1, \dots, N$:

$$\left| \text{SW}_p^p(\tilde{G}_i(\phi, \pi), G_i) - \text{SW}_p^p(\tilde{G}_i(\phi^{(h)}, \pi^{(h)}), G_i) \right| \leq \gamma(\delta), \tag{66}$$

where $\lim_{\delta \rightarrow 0} \gamma(\delta) = 0$. Averaging over i and taking expectation, this implies

$$\frac{1}{N} \sum_{i=1}^N \left| \text{SW}_p^p(\tilde{G}_i(\phi, \pi), G_i) - \text{SW}_p^p(\tilde{G}_i(\phi^{(h)}, \pi^{(h)}), G_i) \right| \leq \gamma(\delta), \text{ and} \quad (67)$$

$$\mathbb{E} \left[\left| \text{SW}_p^p(\tilde{G}(\phi, \pi), G) - \text{SW}_p^p(\tilde{G}(\phi^{(h)}, \pi^{(h)}), G) \right| \right] \leq \gamma(\delta) \quad (68)$$

By Jensen's inequality, we have:

$$\left| \frac{1}{N} \sum_{i=1}^N \text{SW}_p^p(\tilde{G}_i(\phi, \pi), G_i) - \frac{1}{N} \sum_{i=1}^N \text{SW}_p^p(\tilde{G}_i(\phi^{(h)}, \pi^{(h)}), G_i) \right| \leq \gamma(\delta), \text{ and} \quad (69)$$

$$\left| \mathbb{E} \left[\text{SW}_p^p(\tilde{G}(\phi, \pi), G) - \text{SW}_p^p(\tilde{G}(\phi^{(h)}, \pi^{(h)}), G) \right] \right| \leq \gamma(\delta) \quad (70)$$

which is equivalent to

$$|R_N(\phi, \pi) - R_N(\phi^{(h)}, \pi^{(h)})| \leq \gamma(\delta), \text{ and} \quad |R(\phi, \pi) - R(\phi^{(h)}, \pi^{(h)})| \leq \gamma(\delta). \quad (71)$$

Using triangle inequality, we have:

$$\begin{aligned} & \sup_{(\phi, \pi) \in \Phi \times \Delta^K} |R_N(\phi, \pi) - R(\phi, \pi)| \\ & \leq \sup_{(\phi, \pi) \in \Phi \times \Delta^K} \left(|R_N(\phi, \pi) - R_N(\phi^{(h)}, \pi^{(h)})| + |R_N(\phi^{(h)}, \pi^{(h)}) - R(\phi, \pi)| \right) \\ & \leq \sup_{(\phi, \pi) \in \Phi \times \Delta^K} \left(|R_N(\phi, \pi) - R_N(\phi^{(h)}, \pi^{(h)})| + |R_N(\phi^{(h)}, \pi^{(h)}) - R(\phi^{(h)}, \pi^{(h)})| \right. \\ & \quad \left. + |R(\phi^{(h)}, \pi^{(h)}) - R(\phi, \pi)| \right) \\ & \leq \max_{h=1, \dots, H} |R_N(\phi^{(h)}, \pi^{(h)}) - R(\phi^{(h)}, \pi^{(h)})| + 2\gamma(\delta). \end{aligned} \quad (72)$$

Let $Z_N := \sup_{(\phi, \pi) \in \Phi \times \Delta^K} |R_N(\phi, \pi) - R(\phi, \pi)|$ and $A_N^\varepsilon := \{Z_N > \varepsilon\}$, $\varepsilon > 0$. Almost

sure convergence $Z_N \xrightarrow{a.s} 0$ is equivalent to

$$\forall \varepsilon > 0 : \quad \mathbb{P}\left(\limsup_{N \rightarrow \infty} A_N^\varepsilon\right) = 0, \quad (73)$$

where $\limsup_{N \rightarrow \infty} A_N^\varepsilon := \bigcap_{m=1}^{\infty} \bigcup_{N \geq m} A_N^\varepsilon$. For a fixed $\varepsilon > 0$, we choose $\delta > 0$ so small that $2\gamma(\delta) < \varepsilon/2$. Then (72) implies the event inclusion

$$A_N^\varepsilon \subseteq \bigcup_{h=1}^H \left\{ |R_N(\phi^{(h)}, \pi^{(h)}) - R(\phi^{(h)}, \pi^{(h)})| > \frac{\varepsilon}{2} \right\} =: \bigcup_{h=1}^H B_{N,h}^{\varepsilon/2}. \quad (74)$$

Therefore,

$$\limsup_{N \rightarrow \infty} A_N^\varepsilon \subseteq \bigcup_{h=1}^H \left(\limsup_{N \rightarrow \infty} B_{N,h}^{\varepsilon/2} \right). \quad (75)$$

By the strong law of large numbers (using Assumption 3) applied to each fixed $(\phi^{(h)}, \pi^{(h)})$,

$$|R_N(\phi^{(h)}, \pi^{(h)}) - R(\phi^{(h)}, \pi^{(h)})| \xrightarrow{a.s} 0, \quad (76)$$

hence, for every h and every $\eta > 0$,

$$\mathbb{P}\left(\limsup_{N \rightarrow \infty} \{ |R_N(\phi^{(h)}, \pi^{(h)}) - R(\phi^{(h)}, \pi^{(h)})| > \eta \}\right) = 0. \quad (77)$$

Taking $\eta = \varepsilon/2$ and using the finite union bound, we get

$$\mathbb{P}\left(\limsup_{N \rightarrow \infty} A_N^\varepsilon\right) \leq \sum_{k=1}^K \mathbb{P}\left(\limsup_{N \rightarrow \infty} B_{N,k}^{\varepsilon/2}\right) = 0. \quad (78)$$

Since this holds for every $\varepsilon > 0$, it follows that

$$\forall \varepsilon > 0 : \quad \mathbb{P}\left(\limsup_{N \rightarrow \infty} A_N^\varepsilon\right) = 0, \quad (79)$$

which is equivalent to $Z_N \rightarrow 0$ almost surely, i.e.,

$$\sup_{\phi \in \Phi} |R_N(\phi, \pi) - R(\phi, \pi)| \xrightarrow{a.s.} 0, \quad (80)$$

which completes the proof of the uniform law of large numbers for the risks. \square

With the proved uniform law of large numbers, we now discuss the proof of posterior consistency. For all $\epsilon > 0$, we define the “bad” set of parameters:

$$S_\epsilon(\phi_0, \pi_0) := \{(\phi, \pi) \in \Phi \times \Delta^K : \|\phi - \phi_0\|_p + \|\pi - \pi_0\|_p \geq \epsilon\}, \quad (81)$$

where (ϕ_0, π_0) is defined in Assumption 1. Our target is to show that

$$p_N(S_\epsilon(\phi_0, \pi_0)) \xrightarrow{a.s.} 0, \quad (82)$$

for all $\epsilon > 0$ and p_N is our posterior measure. For $\varepsilon > 0$, let

$$A_N := \{p_N(S_\epsilon(\phi_0, \pi_0)) > \varepsilon\}. \quad (83)$$

By the definition of almost sure convergence in terms of the limit superior of events, it suffices to show

$$\mathbb{P}\left(\limsup_{N \rightarrow \infty} A_N\right) = 0, \quad (84)$$

where $\limsup_{N \rightarrow \infty} A_N := \bigcap_{m=1}^{\infty} \bigcup_{N \geq m} A_N$. By the uniform law of large numbers (Lemma 4), for any $\eta > 0$ define the event

$$E_N := \left\{ \sup_{(\phi, \pi) \in \Phi \times \Delta^K} |R_N(\phi, \pi) - R(\phi, \pi)| \leq \eta \right\}. \quad (85)$$

Then E_N occurs eventually almost surely. On E_N :

- For $(\phi, \pi) \in S_\epsilon(\phi_0, \pi_0)$,

$$R_N(\phi, \pi) \geq R(\phi, \pi) - \eta \geq R(\phi_0, \pi_0) + \Delta(\epsilon) - \eta, \quad (86)$$

where $\Delta(\epsilon) = \inf_{\{(\phi, \pi) \in \Phi \times \Delta^K : \|\phi - \phi_0\|_p + \|\pi - \pi_0\|_p \geq \epsilon\}} (R(\phi, \pi) - R(\phi_0, \pi_0)) > 0$ (Assumption 1).

- For $(\phi, \pi) \in B_\delta(\phi_0, \pi_0) := \{(\phi, \pi) : \|\phi - \phi_0\|_p + \|\pi - \pi_0\|_p < \delta\}$ ("good" set), choose δ small so that

$$\sup_{(\phi, \pi) \in B_\delta(\phi_0, \pi_0)} (R(\phi, \pi) - R(\phi_0, \pi_0)) \leq \eta, \quad (87)$$

then

$$R_N(\phi, \pi) \leq R(\phi, \pi) + \eta \leq R(\phi_0, \pi_0) + 2\eta. \quad (88)$$

On E_N , the posterior mass ratio of “bad” set and “good” set

$$\begin{aligned}
\frac{p_N(S_\epsilon(\phi_0, \pi_0))}{p_N(B_\delta(\phi_0, \pi_0))} &= \frac{\int_{S_\epsilon(\phi_0, \pi_0)} \exp(-wNR_N(\phi, \pi)) dp(\phi, \pi)}{\int_{B_\delta(\phi_0, \pi_0)} \exp(-wNR_N(\phi, \pi)) dp(\phi, \pi)} \\
&\leq \frac{p(\Phi \times \Delta^K) \exp(-wN(R(\phi_0, \pi_0) + \Delta(\epsilon) - \eta))}{p(B_\delta(\phi_0, \pi_0)) \exp(-wN(R(\phi_0, \pi_0) + 2\eta))} \\
&= \frac{1}{p(B_\delta(\phi_0))} \exp(-wN(\Delta(\epsilon) - 3\eta)),
\end{aligned} \tag{89}$$

where $p(\phi, \pi)$ is the prior measure. Therefore, we have

$$p_N(S_\epsilon(\phi_0, \pi_0)) \leq C \exp(-wN(\Delta(\epsilon) - 3\eta)), \tag{90}$$

where $C = \frac{1}{\pi(B_\delta(\phi_0, \pi_0))} > 0$ due to Assumption 4. Choose $\eta < \Delta(\epsilon)/4$ so that $\Delta(\epsilon) - 3\eta > \Delta(\epsilon)/4 > 0$, then the right-hand side decays exponentially in N , implying that for almost every sample path ω there exists $N_0(\omega)$ such that for all $N \geq N_0(\omega)$,

$$p_N(S_\epsilon(\phi_0, \pi_0)) < \varepsilon. \tag{91}$$

By the definition of \limsup of events,

$$\limsup_{N \rightarrow \infty} A_N = \bigcap_{m=1}^{\infty} \bigcup_{N \geq m} \{p_N(S_\epsilon(\phi_0, \pi_0)) > \varepsilon\} = \emptyset \quad \text{a.s.} \tag{92}$$

Hence,

$$\mathbb{P}\left(\limsup_{N \rightarrow \infty} A_N\right) = 0. \tag{93}$$

Since the choice of $\varepsilon > 0$ is arbitrary, we conclude

$$p_N(S_\varepsilon(\phi_0, \pi_0)) \xrightarrow{\text{a.s.}} 0. \quad (94)$$

Hence, the posterior concentrates around (ϕ_0, π_0) for any $\varepsilon > 0$, proving Bayesian posterior consistency.

A.4 Convexity of Sliced Wasserstein Barycenter

We discuss the convexity of SWB in the distribution space in the following proposition.

Proposition 1 (Convexity of Sliced Wasserstein Barycenter). *Given $F_1, \dots, F_k, G \in \mathcal{P}_p(\mathbb{R}^d)$ and $(\pi_1, \dots, \pi_K) \in \Delta^K$, the mapping*

$$G \rightarrow \sum_{k=1}^K \pi_k SW_p^p(G, F_k) \quad (95)$$

is convex in G i.e.,

$$\sum_{k=1}^K \pi_k SW_p^p(G_t, F_k) \leq t \sum_{k=1}^K \pi_k SW_p^p(G_0, F_k) + (1-t) \sum_{k=1}^K \pi_k SW_p^p(G_1, F_k), \quad (96)$$

for $G_t = tG_0 + (1-t)G_1$ with $t \in [0, 1]$ and any pair of measures $G_0, G_1 \in \mathcal{P}_p(\mathbb{R}^d)$.

Proof. We first show that $W_p^p(G, F_k)$ is convex with respect to G . Let $G_t = tG_0 + (1-t)G_1$ for $t \in [0, 1]$ and any pair of measures (G_0, G_1) , we define γ_0 as the *optimal* coupling between G_0 and G_k and γ_1 as the *optimal* coupling between G_1 and G_k . Let $\gamma_t = t\gamma_0 + (1-t)\gamma_1$, we

have G_t and F_k be the corresponding two marginals of γ_t . We have:

$$\begin{aligned}
W_p^p(G_t, F_k) &= \inf_{\gamma \in \Pi(G_t, G_k)} \mathbb{E}_{(x,y) \sim \gamma} [\|x - y\|_p^p] \\
&\leq \mathbb{E}_{(x,y) \sim \gamma_t} [\|x - y\|_p^p] \\
&= t \mathbb{E}_{(x,y) \sim \gamma_0} [\|x - y\|_p^p] + (1 - t) \mathbb{E}_{(x,y) \sim \gamma_1} [\|x - y\|_p^p] \\
&= t W_p^p(G_0, F_k) + (1 - t) W_p^p(G_1, F_k).
\end{aligned} \tag{97}$$

Next, we show that $\text{SW}_p^p(G, F_k)$ is also convex with respect to G . Using the proved convexity of the Wasserstein distance, we have:

$$\begin{aligned}
\text{SW}_p^p(G_t, F_k) &= \mathbb{E}_{\theta \sim \mathcal{U}(\mathbb{S}^{d-1})} [W_p^p(\theta \sharp G_t, \theta \sharp F_k)] \\
&\leq \mathbb{E}_{\theta \sim \mathcal{U}(\mathbb{S}^{d-1})} [W_p^p(\theta \sharp t G_0, \theta \sharp F_k) + W_p^p(\theta \sharp (1-t) G_1, \theta \sharp F_k)] \\
&= t \text{SW}_p^p(F_0, G_k) + (1 - t) \text{SW}_p^p(F_1, G_k).
\end{aligned} \tag{98}$$

Since $\sum_{k=1}^K \pi_k \text{SW}_p^p(G, F_k)$ is a positive weighted sum of $\text{SW}_p^p(G, F_k)$, it is also convex with respect to G . \square

B Additional Results

As mentioned in the main text, we show the observed responses and the posterior means of the KDEs of the fitted DDR and MDDR distributions for NK cells and Monocytes in Figure 4. From these figures, MDDR again led to better fits than DDR for both training and testing donors.

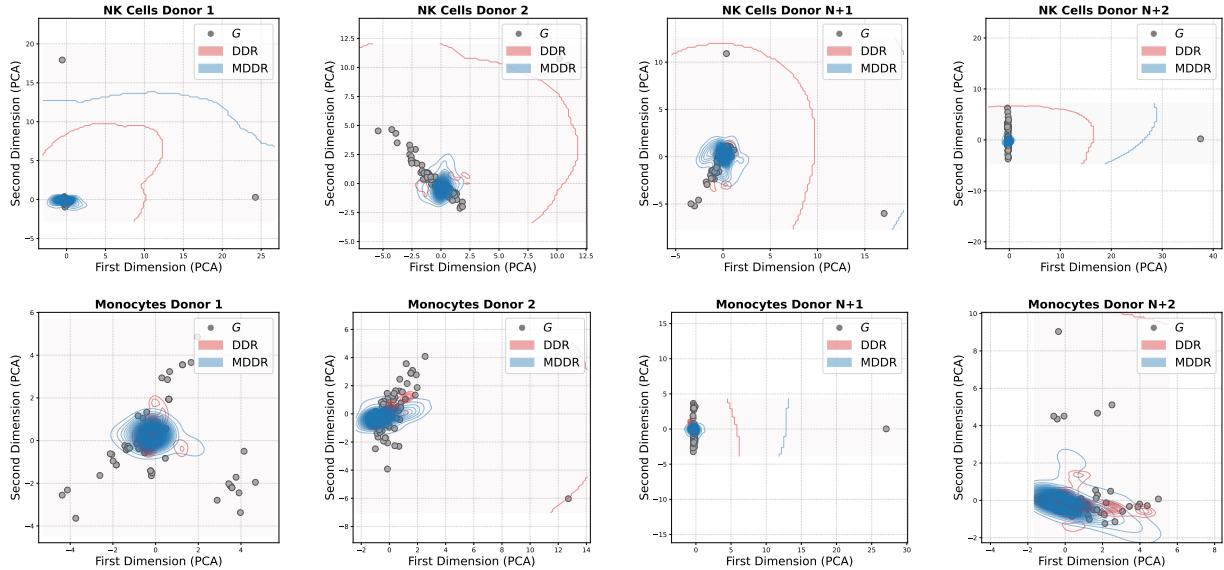


Figure 4: The first two columns show two random in-sample donors and the last two columns show two random out-sample donors. The first row presents results for NK Cells including the observed responses, and the posterior means of the KDEs of fitted distributions of DDR and MDDR. The second row presents similar results for Monocytes.